



1 Carbon dynamics at the river-estuarine transition: a comparison among tributaries
2 of Chesapeake Bay.

3 Paul A. Bukaveckas
4 Center for Environmental Studies
5 Virginia Commonwealth University

8 Corresponding author: Paul Bukaveckas (pabukaveckas@vcu.edu)

9 Keywords: carbon, estuaries, mass balance CO₂ flux

10



11 Abstract

12 Sources and transformation of C were quantified using mass balance and ecosystem metabolism
13 data for the upper segments of the James, Pamunkey and Mattaponi Estuaries. The goal was to
14 assess the role of external (river inputs & tidal exchange) vs. internal (metabolism) drivers in
15 influencing the forms and fluxes of C. C forms and their response to river discharge differed
16 among the estuaries based on their physiographic setting. The James, which receives the bulk of
17 inputs from upland areas (Piedmont and Mountain), exhibited a higher ratio of inorganic to
18 organic C, and larger inputs of POC. The Pamunkey and Mattaponi receive a greater proportion
19 of inputs from lowland (Coastal Plain) areas, which were characterized by low DIC and POC,
20 and elevated DOC. We anticipated that transport processes would dominate during colder
21 months when discharge is elevated and metabolism is low, and that biological processes would
22 predominate in summer, leading to attenuation of C through-puts via de-gassing of CO₂.
23 Contrary to expectations, highest retention of OC occurred during periods of high through-put, as
24 elevated discharge resulted in greater loading and retention of POC. In summer, internal cycling
25 of C via production and respiration was large in comparison to external forcing despite the large
26 riverine influence in these upper estuarine segments. The estuaries were found to be net
27 heterotrophic based on retention of OC, export of DIC, low GPP relative to ER, and a net flux of
28 CO₂ to the atmosphere. In the James, greater contributions from phytoplankton production
29 resulted in a closer balance between GPP and ER, with autochthonous production exceeding
30 allochthonous inputs. Combining the mass balance and metabolism data with bioenergetics
31 provided a basis for estimating the proportion of C inputs utilized by the dominant metazoan.
32 The findings suggest that invasive catfish utilize 15% of total OM inputs and up to 40% of
33 allochthonous inputs to the James.

34 Non-technical summary: Inland waters play an important role in the global carbon cycle by
35 storing, transforming and transporting carbon from land to sea. Comparatively little is known
36 about carbon dynamics at the river-estuarine transition. A study of tributaries of Chesapeake
37 Bay showed that biological processes exerted a strong effect on carbon transformations. Peak
38 carbon retention occurred during periods of elevated river discharge and was associated with
39 trapping of particulate matter.



40 1. Introduction

41 Inland waters occupy a small proportion of surface area but play a disproportionately large role
42 in global C cycling (Cole et al. 2007; Butman et al. 2016; Tranvik et al. 2018; Holgerson and
43 Raymond 2016). River networks act as transport systems delivering C products of mineral
44 weathering (DIC) and plant decomposition (DOC, POC) from the terrestrial realm to the coastal
45 ocean (Meybeck 2003). Inland waters also function as reactors in which biotic and abiotic
46 processes act to augment, transform or attenuate C fluxes. Aquatic primary production
47 supplements terrestrial DOC and POC inputs, and by providing more labile forms of C, may
48 facilitate the decomposition of older, recalcitrant terrestrial C. Decomposition of aquatic and
49 terrestrial organic matter returns C to the atmosphere, which, along with C sequestration via
50 sediment burial, results in the attenuation of C fluxes to the coastal zone (Richey et al. 2002;
51 Vorosmarty et al. 2003; Middelburg and Herman 2007; Tranvik et al. 2009). Acting against
52 these processes are fluvial forces that hasten through-puts of C and favor transport over
53 processing. Along the flowpath from mountains to the sea, aquatic systems differ greatly in their
54 capacity to attenuate C fluxes depending on factors such as water residence time, ecosystem
55 metabolism and capacity for sediment accrual. Biological processes are expected to exert a
56 stronger influence over C transport in lakes relative to streams and rivers, owing to their longer
57 water residence time (Hotchkiss et al. 2018). Current efforts focus on understanding the net
58 effect of inland waters on landscape scale fluxes of C. In this context, comparatively little
59 attention has been focused on processes occurring at the river-estuarine transition.

60 The river-estuarine ecotone is defined by the transition from fluvial- to tidal-dominated forces,
61 which results in a shift from unidirectional to bidirectional flow. In some settings, the point of
62 transition may migrate in response to changing discharge conditions, with fluvial forces
63 extending seaward during high discharge, and tidal forces gaining inland during periods of low
64 freshwater inputs. Along the mid-Atlantic coast, the landward extent of tidal influence is
65 delineated by a geologic feature (the Fall Line), a zone of rapid elevation change at the transition
66 from upland (Piedmont) to lowland (Coastal Plain) physiographic regions. Below the Fall Line,
67 hydrodynamics are estuarine in that they are subject to bi-directional flows associated with
68 incoming and outgoing tides, whereas chemistry is riverine (freshwater). These conditions arise
69 because tidal forces propagate inland beyond the point where mixing of fresh and marine waters



70 occurs. Tidal freshwaters are a common feature of river-dominated estuaries throughout the
71 world but have received relatively little attention in landscape-scale assessments of
72 biogeochemical processes (Hoitink and Jay 2016; Ward et al. 2017; Jones et al. 2020). A key
73 feature of tidal freshwaters is their prolonged residence time relative to non-tidal rivers. Water
74 and materials exported during an out-going tide are returned on the incoming tide, thereby
75 increasing residence time. For example, plankton community development in rivers is often
76 constrained by short transit time (Soballe and Kimmel 1987; Pace et al. 1992; Basu and Pick
77 1996; Sellers and Bukaveckas 2003; Lucas et al. 2009), whereas the back and forth of tidal flows
78 reduces net seaward movement resulting in longer residence time (Shen and Lin 2006; Qin and
79 Shen 2017). Bi-directional flows in tidal freshwaters create more favorable water residence time
80 conditions (relative to non-tidal rivers) that allow for the development of phytoplankton
81 communities and the potential for greater biological influence on C forms and retention. Our
82 prior work in the James Estuary has documented higher rates of ecosystem metabolism in the
83 tidal freshwater segment relative to adjacent riverine and lower estuarine segments (Tassone and
84 Bukaveckas 2019; Bukaveckas et al. 2020). The occurrence of a chlorophyll-a and productivity
85 maxima in the tidal fresh zone was attributed to longer water residence time and proximal
86 nutrient inputs from riverine and local point sources (Bukaveckas et al. 2011; Qin and Shen
87 2017). Other studies have also documented tidal freshwaters as potential biogeochemical
88 hotspots (Vincent et al. 1996; Muylaert et al. 2005; Hoffman et al. 2008; Lionard et al. 2008;
89 Amann et al. 2015; Young et al. 2021).

90 The goal of this study was to assess the relative importance of external (river inputs & tidal
91 exchange) vs. internal (metabolism) drivers in influencing C forms and retention in the upper
92 estuary. Long water residence time and high rates of ecosystem metabolism in the tidal fresh
93 zone were expected to favor the importance of internal processes over external hydrologic forces
94 in regulating C throughputs. During periods of low river discharge, longer water residence in the
95 estuary allows accrual of phytoplankton biomass and greater GPP, which may result in net
96 export of organic C. Alternatively, the production of autochthonous labile C may facilitate
97 mineralization of allochthonous C inputs (“priming effect”) resulting in CO₂ release and
98 attenuation of organic and total C exports (Bianchi 2011; Steen et al. 2015; Ward et al. 2016).
99 During periods of elevated discharge, freshwater replacement time in the upper estuary is short,
100 thereby favoring transport over retention. However, our recent work has shown that the bulk of

101 N and P retention in the tidal fresh zone of the James Estuary occurs during periods of high
102 sediment loading (Bukaveckas et al. 2018). Although retention of dissolved N and P was highest
103 during peak production in summer, the trapping of particulate N and P in winter accounted for
104 the bulk of total N and P retention. These findings suggest that retention of particulate and total
105 C may be highest during periods of elevated river discharge.

106 In this study, mass balance results and ecosystem metabolism data were used to assess C inputs,
107 outputs, transformation and retention in the upper estuarine segments of two Chesapeake Bay
108 tributaries. For the James Estuary, these data are also used to estimate allochthonous and
109 autochthonous inputs and to assess constraints on food web energetics.

110

111 2. Methods

112 2.1 Study Sites. This study focuses on the upper segments of the two southern tributaries of
113 Chesapeake Bay (James and York Estuaries), the latter of which is comprised of two sub-
114 estuaries (Pamunkey and Mattaponi). This is the third in a series of papers that rely in part on
115 comparisons among these estuaries to draw inferences about processes occurring at the river-
116 estuarine transition. Previous papers focused on the influence of storm events on river and
117 estuarine metabolism and water quality (Bukaveckas et al. 2020), and on factors regulating water
118 clarity and primary production (Henderson & Bukaveckas 2021). The proximity of the estuaries
119 facilitated frequent sampling (1-2 week intervals) that is needed to characterize C fluxes. A key
120 difference among the estuaries is their geographic setting across lowland (Coastal Plain) and
121 upland (Piedmont and Mountain) areas (Figure 1). Our study reach within the James Estuary is
122 the tidal fresh segment, for which freshwater inputs are largely (90%) derived from upland
123 sources (as measured by USGS gauging stations at the Fall Line of the James and Appomattox
124 Rivers). Based on contributing area, we estimate that local (Coastal Plain) tributaries entering
125 below the Fall Line contribute ~10% of freshwater inputs to the James tidal fresh segment. By
126 contrast the Pamunkey and Mattaponi Estuaries receive a greater proportion of freshwater inputs
127 from local (Coastal Plain) sources (36% and 51%, respectively). We expected that higher
128 sediment yield from upland sources would result in greater POC inputs to the James relative to
129 the Pamunkey and the Mattaponi. The estuaries also differ in rates of metabolism and forms of
130 primary production. We expected that higher GPP and R in the phytoplankton-dominated James



131 Estuary would exert a stronger influence on C transformations relative to the Pamunkey and
132 Mattaponi, which are dominated by submerged and emergent aquatic vegetation. Lastly, we
133 expected that extensive floodplain and wetland areas along the Pamunkey and Mattaponi would
134 result in greater DOC inputs relative to the James.

135 2.2 Data Collection. For the James, we are able to present a relatively complete C budget
136 inclusive of Fall Line loads, local tributary inputs and tidal fluxes of inorganic and organic
137 fractions (DIC, DOC, POC). These results are based on data collected from river and estuarine
138 stations over a 10-year span (2010-2019). For the Pamunkey and Mattaponi, our scope is more
139 limited both in the time span over which data were collected (2017-2019) and, because we lack
140 data on Fall Line DIC and chloride inputs, and therefore cannot estimate tidal exchange using Cl
141 mass balance. For the James and Pamunkey, we use previously published estimates of GPP and
142 ER derived from in situ diel oxygen cycles to assess their effect on C transformations. For all
143 three estuaries, we characterized seasonal patterns in CO₂ concentrations and atmospheric losses
144 of CO₂.

145 2.3 C Inputs & Estuarine Export. External C loads for the three estuaries were derived from (a)
146 measured discharge and concentration at the Fall Line, and (b) estimated contributions from
147 ungauged tributaries below the Fall Line. Fall Line loads were based on data collected by the
148 USGS at gauging stations located on the James, Pamunkey and Mattaponi Rivers.
149 Approximately 200 measurements of DOC and POC were obtained at each of the gauging sites
150 over the 10-year span (**Table 1**), along with continuous measurements of river discharge. For the
151 James, we supplemented these data by measuring DIC and Cl at the Fall Line during 2012-2019
152 (189 observations). We modeled seasonal, inter-annual and discharge-dependent variation in
153 riverine C concentrations using Generalized Additive Models (see Statistics). The models were
154 used to predict daily concentrations at each site, and, in combination with daily discharge, to
155 derive daily loading values at the Fall Line. We estimated the local (ungauged) runoff based on
156 the proportion of catchment area represented by tributaries entering below the Fall Line. The
157 inferred ungauged discharge was derived as a constant fraction of the daily Fall Line discharge.
158 Measurements of C concentrations obtained from a Coastal Plain tributary of the James Estuary
159 (Kimages Creek; Bukaveckas and Wood 2014) were used to represent the chemistry of runoff
160 below the Fall Line. Kimages Creek was sampled twice monthly for DOC, POC and DIC during



161 2012-19 (211 observations). These data were modeled (GAM) to capture seasonal and inter-
162 annual patterns in C concentrations. GAM-predicted values were used to infer daily
163 concentrations and, along with the estimated discharge entering below the Fall Line, to derive
164 daily inputs from ungauged tributaries for each of the estuaries. Total loads inclusive of Fall
165 Line and ungauged inputs were normalized per unit area of the estuary and presented as monthly
166 averages of daily values (e.g., g DOC m⁻² d⁻¹).

167 Estuarine export is the mass of C lost due to displacement of estuarine waters by catchment
168 runoff. Estuarine export was derived as the product of total runoff (Fall Line and ungauged
169 discharge) and estuarine C concentrations at stations located at the seaward end of our study
170 reaches (JMS69, PMK6, MPN4; [Table 1](#)). Estuarine C concentrations were modeled (GAMs) to
171 capture seasonal, inter-annual and discharge-dependent variation. GAM-predicted values were
172 used to infer daily estuarine C concentrations and, in combination with discharge, to derive daily
173 estimates of estuarine C export. Exports are presented as monthly averages of daily values
174 normalized per unit area of the estuary.

175 2.4 Tidal Fluxes & Estuarine Retention. Tidal exchange is the process by which incoming and
176 outgoing tides may deplete or enrich chemical constituents in the estuary depending on the
177 strength and direction of chemical gradients across the exchange boundary. The volume of tidal
178 exchange is rarely measured directly, and therefore conservative tracers (e.g., chloride) are
179 typically used to estimate tidal fluxes (Robson et al. 2008; Bukaveckas & Isenberg 2013). The
180 Cl mass balance approach yields an estimate of the effective tidal exchange (i.e., the net
181 difference in mass flux between incoming and outgoing tides). In practical terms, it is the
182 amount of Cl needed to balance the budget taking into account (a) riverine inputs of Cl (Fall Line
183 plus local tributaries), (b) estuarine export of Cl, and (c) the observed change in mass of Cl
184 within the estuary. Cl concentrations in the James were monitored along with riverine Cl (at the
185 Fall Line) and our proxy tributary representing ungauged inputs below the Fall Line (Kimages
186 Creek). Similar to the derivation of C fluxes, we used GAM models to generate predicted daily
187 Cl concentrations for the river (Fall Line) and local tributary based on seasonal, inter-annual and
188 discharge-dependent variation. Daily concentrations were used in combination with Fall Line
189 discharge, below Fall Line discharge, and total discharge to derive daily input and export fluxes.
190 Daily fluxes were summed over the budget interval (typically 1-2 weeks) and used, in



191 conjunction with the change in mass of Cl in the estuary between the start and end of each
192 interval, to solve for the net tidal flux of Cl.

$$193 \quad \text{Estuary Cl Mass}_{t+1} = \text{Estuary Cl Mass}_t + \text{Riverine Cl} - \text{Export Cl} \pm \text{Net Tidal Cl} \quad (1)$$

194 The mass of Cl required to balance each budget interval was used in combination with
195 measurements of Cl concentrations in tidal inflow and outflow, as represented by stations located
196 on either side of the seaward boundary of our study reach (JMS69 and JMS56), to derive the
197 effective volume of tidal exchange. This represents the volume of “new” water entering the
198 study reach from the lower estuary with each tidal cycle. The James has an elongate shape that
199 is typical of estuaries that occupy flooded river valleys. The back and forth of tidal flows means
200 that the bulk of the water leaving on an outgoing tide returns on the subsequent incoming tide,
201 and only a small proportion of the large tidal flux is “new” water. For the James, we have
202 previously estimated that the effective volume of exchange is equivalent to 8% of the tidal prism
203 (Bukaveckas and Isenberg 2013). For this study, estimates of the volume of tidal exchange were
204 derived for each budget interval (N = 309 for 2011-19). The effective volume of exchange was
205 used along with measured C concentrations of tidal inflows and outflows to determine the net
206 exchange of C at the seaward boundary of the study reach. Net tidal fluxes for each budget
207 interval were aggregated to monthly values and presented as daily areal values for comparison to
208 riverine input and export fluxes. Lastly, we derived monthly estimates of estuarine C retention
209 based on the difference between input and output fluxes taking into account changes in mass
210 storage within the estuary.

$$211 \quad \text{Estuary C Mass}_{t+1} = \text{Estuary C Mass}_t + \text{Riverine C} - \text{Export C} \pm \text{Net Tidal C} \pm \text{Retention} \quad (2)$$

212 For DIC, our estimation of retention also took into account air-water CO₂ exchange (see below).

213 2.5 Estuarine Metabolism. To assess the role of internal C transformations via photosynthesis
214 and respiration, we used our previously published estimates of GPP and ER for the James and
215 Pamunkey (Bukaveckas et al. 2020). Rates of metabolism were derived from continuous (15
216 min) monitoring of dissolved oxygen at stations located within our study segments of the James
217 and Pamunkey (Figure 1). The James monitoring station is located at the VCU Rice Center
218 Research Pier, approximately 2 km from our JMS75 sampling location. The Pamunkey station
219 (White House Landing) is operated by the Virginia Institute of Marine Science and located near

220 the mid-point of our study segment. Similar equipment (YSI 6600 or EXO sondes) and
221 protocols are used at the two stations including routine (2-3 week) maintenance and calibration
222 of sondes as per manufacturer recommendations. Daily GPP and ER were derived using the
223 single-station open-water method. Following Caffrey (2003; 2004), 15-minute DO
224 measurements were smoothed to 30-minute averages and multiplied by water depth to obtain
225 areal rates of oxygen flux at 30 minute intervals throughout the day.

226
$$\text{O}_2 \text{ flux (g O}_2 \text{ m}^{-2} \text{ d}^{-1}) = (\text{DO}_{t2} - \text{DO}_{t1}) * \text{Water Depth} - \text{AE} \quad (3)$$

227 Atmospheric exchange (AE) was derived at 30-minute intervals based on water column DO
228 saturation and a generic estuarine gas transfer coefficient. We have previously analyzed 23 years
229 of station data for the James and found that estimates of atmospheric exchange derived from
230 oxygen saturation and the fixed gas transfer coefficient were not significantly different from
231 exchange coefficients derived using variable water velocity and wind speed (Tassone and
232 Bukaveckas 2019). ER was derived by extrapolating nightly O₂ fluxes to a 24-hour period. GPP
233 was derived as the sum of daytime oxygen production and ER during daylight hours. Oxygen-
234 based values were converted to C assuming a PQ of 1.2 and RQ of 1.

235 2.6 Sampling and Analysis. Methods were described previously (Bukaveckas et al. 2011;
236 Bukaveckas et al. 2020; Henderson and Bukaveckas 2021) and are summarized here. Data were
237 collected from 4 stations in the James tidal fresh segment, 3 stations in each of the Pamunkey
238 and Mattaponi study reaches, and one tributary stream (Kimages Creek) located at the VCU Rice
239 Center (Figure 1; Table 1). Estuarine sites were sampled by boat in the main channel except in
240 the upper, narrow sections of the Pamunkey and Mattaponi where samples were collected from
241 shore in areas of active flow. Owing to vertically well-mixed conditions (no temperature or
242 salinity stratification) water samples and in situ measurements were obtained near the surface
243 (~0.5 m). Water temperature and salinity were measured using a YSI Pro DDS sonde. The
244 partial pressure of carbon dioxide in water and air was measured in the field using a PP Systems
245 EGM 4 portable infrared CO₂ analyzer calibrated at 0 and 2000 ppm. Water samples were
246 analyzed for chlorophyll-a (CHLa), POC, DIC, DOC and Cl. Samples for CHLa and POC were
247 filtered through Whatman GF/A glass filters (0.5-µm nominal pore size). Filters for CHLa
248 analyses were extracted for 18 h in buffered acetone and analyzed on a Turner Design TD-700
249 Fluorometer (Arar and Collins 1997). Filters for POC analysis were dried at 60 C for 48 h,



250 fumed with HCl to remove inorganic carbon and analyzed on a Perkin–Elmer CHN analyzer.
251 Chloride concentrations were determined using a Skalar segmented flow analyzer by the
252 ferricyanide method (APHA 1998). Samples for DIC and DOC were filtered in the field
253 through Whatman GF/A filters and analyzed using a Shimadzu TOC analyzer.

254 2.7 Air-Water CO₂ Fluxes. Air-water exchange of CO₂ was calculated using the equation from
255 Cai and Wang (1998):

$$256 \text{ Flux CO}_2 = K_T K_H (p\text{CO}_{2\text{-water}} - p\text{CO}_{2\text{-air}}) \quad (4)$$

257 where K_T is the gas transfer velocity, K_H is the solubility constant and $p\text{CO}_2$ is the partial
258 pressure of CO₂ in water and air. The solubility constant was derived according to the equation
259 of Weiss (1974) taking into account water temperature and salinity recorded at the time of CO₂
260 measurement. Gas transfer velocities were initially derived from daily average wind speed (U10
261 corrected) measured at the VCU Rice Center Research Pier (James) and the Taskinas Creek
262 NERR station (Pamunkey and Mattaponi). Gas transfer velocities derived from wind speed
263 generally fell within the range of 1 to 1.5 m d⁻¹, which is low in comparison to the global average
264 (5.7 m d⁻¹, Raymond et al. 2017) and to values that are considered appropriate for large rivers
265 (4.3 m d⁻¹, Alin et al. 2011; Reiman and Xu 2019). Wind speeds were low in the upper segments
266 of these estuaries because the prevailing winds (SSW) are nearly perpendicular to the long axis
267 of the channel, which runs mostly east-west. Turbulence generated by strong tidal forces in
268 shallow channels likely plays a greater role in influencing boundary conditions for gas exchange
269 (Raymond and Cole 2001; Borges et al. 2004). We feel that these conditions support the use of
270 higher exchange coefficients than would be derived from wind speed alone and therefore used a
271 value of 4.3 m d⁻¹ for all calculations.

272 2.8 Statistics. Generalized Additive Models (GAMs) were used to model river and estuarine C
273 and Cl concentrations based on discharge, day of year (to capture seasonal patterns) and decimal
274 date (to depict inter-annual variation). GAMs are gaining increasing usage for modeling water
275 chemistry due to their ability to account for non-linear effects and to fit trends of a form that is
276 not known *a priori* (Morton & Henderson 2008; Murphy et al. 2019; Yang and Moyer 2020;
277 Wiik et al. 2021). The GAM analysis was performed using the "mgcv" package in R (Wood
278 2006). The package default thin plate regression spline was used to depict the effect sizes of
279 discharge and decimal date; a cyclic cubic regression spline was used to depict seasonal effects.



280 The default output for the effect size was shifted to center on the mean of the modeled dependent
281 variable to show the response of the GAM model within the range of dependent variable values.

282

283 3. Results

284 3.1 Estuarine Hydrology

285 The James, Pamunkey and Mattaponi Rivers exhibit similar hydrographs with highest monthly
286 average discharge during January-May and lowest discharge in July-November (Figure 2).
287 Average monthly discharge in winter-spring is approximately 4-fold higher in comparison to
288 summer-fall. Median freshwater replacement times (FRT), taking into account Fall Line inputs
289 plus local (ungauged) tributaries, were 30 d (James), 46 d (Mattaponi) and 60 d (Pamunkey)
290 during the period of study. The mass of Cl in the James tidal fresh segment varied by >20-fold
291 from seasonal minimum values during high discharge (~7 mg L⁻¹) to peak values (>100 mg L⁻¹)
292 during summer base flow (Figure 3). Despite the large seasonal variation, Cl changed relatively
293 slowly within the estuary (median = 0.5 % d⁻¹). The gradual change in estuarine Cl belies the
294 underlying dynamics in which input and output fluxes largely offset. Riverine inputs (Fall Line
295 plus local) ranged from 1 to 3 g Cl m⁻² d⁻¹ over the seasonal cycle. These displaced a larger mass
296 of Cl (export = 2-5 g Cl m⁻² d⁻¹) owing to higher Cl concentrations in the estuary relative to river
297 inputs. In late summer (August-October), the development of strong Cl gradients across the
298 seaward boundary of the study reach resulted in high rates of Cl gain and loss via tidal exchange
299 (up to 10-20 g Cl m⁻² d⁻¹). As the lower tidal fresh segment accounts for the bulk of total volume
300 (80%), increases in Cl at the seaward end of the study reach had a large effect on estuarine Cl
301 mass. These seasonal increases in estuarine Cl were most pronounced in summers with low
302 freshwater inputs (e.g., 2012, 2017, 2019). By volume, the effective tidal exchange derived from
303 the Cl mass balance was equivalent to 7.4% (median) and 14 ± 1% (mean and SE) of the tidal
304 prism.

305 3.2 Discharge Effects on River and Estuarine C

306 Discharge was a significant factor influencing riverine C concentrations, though the strength of
307 these effects differed among C fractions and among the three tributaries. Increasing discharge
308 was associated with increasing river DOC in the Mattaponi (from 6 to 12 mg L⁻¹) and Pamunkey



309 (from 5 to 9 mg L⁻¹), but had little effect on James River DOC, which was generally low over the
310 range of observed discharge (3-4 mg L⁻¹; [Figure 4](#)). Generalized Additive Models incorporating
311 discharge, seasonal and inter-annual variation accounted for 50 to 81% of the variation in river
312 DOC ([Table 2](#)). Seasonal patterns were characterized by peak river DOC in summer and
313 minimum values in spring, with a seasonal range of 2-3 mg L⁻¹ ([Supplemental Figure 1](#)). For
314 POC, increasing discharge was associated with large increases in the James River (from 1 to 20
315 mg L⁻¹). Discharge accounted for the bulk of the variation in James River POC (71%) with little
316 additional variation explained by season or inter-annual effects (76% for full model). The effects
317 of discharge on river POC were weaker in the Mattaponi and Pamunkey, where concentrations
318 were generally low over the range of discharge (<2 and <4 mg L⁻¹, respectively). Models
319 incorporating discharge, seasonal and inter-annual variation accounted for 38% and 51%
320 (respectively) of the variation in river POC at these sites ([Supplemental Figure 2](#)). Increasing
321 discharge was associated with large decreases in DIC of the James River (from 20 to 1 mg L⁻¹).
322 The GAM analysis accounted for 44% of the variation in DIC at this site (no river DIC data for
323 Pamunkey and Mattaponi). Overall, increasing discharge resulted in higher DOC concentrations
324 in the Pamunkey and Mattaponi Rivers, higher POC concentrations in the James River, and
325 lower DIC concentrations in the James River.

326 Although increases in discharge had a positive effect on riverine DOC and POC, estuarine
327 concentrations were only weakly, and in some cases negatively affected by increasing discharge
328 ([Figure 5](#)). In the James, estuarine DOC concentrations were typically higher than riverine
329 values ([Supplemental Figure 3](#)), such that increases in river discharge resulted in a reduction in
330 estuarine DOC (from 7 to 2 mg L⁻¹). In the Pamunkey and Mattaponi, increasing discharge had
331 little effect on estuarine DOC as estuarine concentrations were similar to river concentrations.
332 Discharge was not a significant predictor of variation in DOC for the Pamunkey and Mattaponi
333 Estuaries ([Table 2](#)). Seasonal and inter-annual effects were also weak, resulting in a low
334 proportion of variation in estuarine DOC explained by the GAMs (13-27%). Similar findings for
335 POC showed weak seasonal, inter-annual and discharge dependent effects and a low proportion
336 of explained variation for the Pamunkey and Mattaponi Estuaries (40% and 14%, respectively).
337 In contrast, POC concentrations in the James Estuary were strongly influenced by season, with
338 predicted concentrations rising from 1 to 2 mg L⁻¹ during winter to summer. POC concentrations
339 were negatively related to discharge, declining by ~0.5 mg L⁻¹ over the lower range of discharge



340 (up to $400 \text{ m}^3 \text{ s}^{-1}$). The overall model accounted for 75% of the variation in POC for the James
341 Estuary. Increasing discharge had a significant negative effect on DIC in all three estuaries,
342 which decreased by $5\text{-}6 \text{ mg L}^{-1}$ over the observed range of discharge. Seasonal and inter-annual
343 effects on estuarine DIC were weaker; the full models accounted for 68-76% of the variation in
344 estuarine DIC. Overall, these findings show that river discharge had strong negative effects on
345 estuarine DIC, but little influence on estuarine DOC and POC. Significant seasonal variation in
346 POC was observed in the James, but not the Pamunkey or Mattaponi.

347 3.3 Estuarine pCO_2

348 GAM analysis revealed significant seasonal and discharge-dependent variation in estuarine pCO_2
349 (Table 2). The effects of discharge on estuarine pCO_2 differed among the 3 tributaries (Figure
350 6). In the Pamunkey and Mattaponi, there was little effect of discharge, except in the upper
351 quartile of the range, which was associated with rising estuarine pCO_2 . In the James, estuarine
352 pCO_2 increased linearly over the lower one-third range of discharge, and thereafter plateaued.
353 The Mattaponi and Pamunkey exhibited large seasonal variations in estuarine pCO_2 . Peak
354 summer concentrations ($\sim 2600 \text{ ppmv}$) were two-fold higher in comparison to winter minimum
355 values ($\sim 1200 \text{ ppmv}$). A more complex seasonal pattern was observed in the James with bi-
356 model peaks in spring and fall (850 and 1250 ppmv , respectively) bracketing low concentrations
357 in mid-summer. In summer, significantly lower pCO_2 was observed at sites located at the CHLa
358 maximum (JMS75 = 789 ppmv , JMS69 = 644 ppmv) relative to stations in the upper tidal fresh
359 segment (JMS99 = 1007 ppmv) and the most seaward station (JMS56 = 909 ppmv ; $p < 0.01$).
360 The two stations located at the CHLa maximum were the only sites to exhibit periodic under-
361 saturation of pCO_2 (Supplemental Figure 4). The low values at these stations were not observed
362 in winter. There was little longitudinal variation in pCO_2 among stations in the Pamunkey and
363 Mattaponi. Overall, annual average concentrations in the Pamunkey ($2010 \pm 117 \text{ ppmv}$) and
364 Mattaponi ($1900 \pm 120 \text{ ppmv}$) were more than 2-fold higher relative to the James (784 ± 77
365 ppmv). Higher pCO_2 concentrations in the Pamunkey and Mattaponi estuaries were associated
366 with larger air-water CO_2 fluxes (2.97 ± 0.17 and $2.77 \pm 0.17 \text{ g C m}^{-2} \text{ d}^{-1}$, respectively) relative
367 to the James ($0.87 \pm 0.05 \text{ g m}^{-2} \text{ d}^{-1}$; Figure 7). Strong seasonal patterns were observed in the
368 Pamunkey and Mattaponi with monthly average fluxes ranging from $1\text{-}2 \text{ g m}^{-2} \text{ d}^{-1}$ in winter to 3-
369 $4 \text{ g m}^{-2} \text{ d}^{-1}$ in summer, whereas fluxes from the James were similar year-round ($\sim 1 \text{ g m}^{-2} \text{ d}^{-1}$).



370 3.4 C Fluxes & Retention

371 C fluxes into and out of the James Estuary varied seasonally (Figure 8). DOC inputs followed
372 expected seasonal patterns with peak values ($1\text{--}2\text{ g m}^{-2}\text{ d}^{-1}$) during months with elevated
373 discharge (January-May) and minimum values ($\sim 0.3\text{ g m}^{-2}\text{ d}^{-1}$) during predominantly low
374 discharge in July-November. Seasonal variation in DOC inputs was closely matched by export
375 fluxes. Net tidal fluxes were negligible by comparison ($-0.03 \pm 0.01\text{ g m}^{-2}\text{ d}^{-1}$) owing to small
376 differences in concentration across the segment boundary. Monthly DOC retention ranged from
377 -0.30 to $0.12\text{ g m}^{-2}\text{ d}^{-1}$, and was generally negative, indicating net export of DOC. On an annual
378 basis, the DOC balance was $-0.10 \pm 0.02\text{ g m}^{-2}\text{ d}^{-1}$, with export exceeding inputs by $11 \pm 5\%$.
379 Riverine inputs of POC varied seasonally with highest values in January-May (0.5 to $1.9\text{ g m}^{-2}\text{ d}^{-1}$)
380 and generally low values in June-December ($< 0.3\text{ g m}^{-2}\text{ d}^{-1}$). By contrast, estuarine export of
381 POC was consistently low throughout the year ($< 0.5\text{ g m}^{-2}\text{ d}^{-1}$). As a result, POC retention was
382 highest in January-May (0.3 to $1.5\text{ g m}^{-2}\text{ d}^{-1}$). Net tidal fluxes were positive indicating a loss of
383 POC with each tidal cycle, but these fluxes were small ($0.09 \pm 0.03\text{ g m}^{-2}\text{ d}^{-1}$) in comparison to
384 river inputs. On an annual basis, the net retention of POC was $0.59 \pm 0.11\text{ g m}^{-2}\text{ d}^{-1}$,
385 corresponding to $72 \pm 4\%$ of inputs. DIC input and output fluxes followed a similar pattern as
386 for DOC, with peak values in months with high discharge. Taking into account estuarine export
387 and atmospheric fluxes, the James was a net source of DIC with losses ($4.25\text{ g m}^{-2}\text{ d}^{-1}$) exceeding
388 inputs ($2.82\text{ g m}^{-2}\text{ d}^{-1}$) by 51% .

389 Our mass balance analysis does not explicitly consider the role of point source inputs as part of
390 the estuarine C budget. Point sources that discharge to the tidal fresh segment of the James are
391 principally wastewater treatment plants, and some industries associated with the Richmond
392 metro area. The volume of effluent discharged to the James is small (annual average = $15\text{--}21\text{ m}^3$
393 s^{-1} during 2007-14) in comparison to annual average river discharge ($\sim 225\text{ m}^3\text{ s}^{-1}$). But as
394 effluent may contain elevated C concentrations, point sources could potentially contribute an
395 appreciable fraction of C inputs. Point sources typically do not report C concentrations as part of
396 their effluent monitoring, therefore we carried out a 2-year study of DIC, DOC and POC
397 concentrations in effluent from the largest point source (City of Richmond WWTP). Effluent
398 POC concentrations ($1.54 \pm 0.13\text{ mg L}^{-1}$) were comparable to riverine values, whereas effluent
399 DOC ($13.1 \pm 1.2\text{ mg L}^{-1}$) and DIC ($22.7 \pm 1.6\text{ mg L}^{-1}$) were two-fold higher relative to riverine



400 concentrations. We extrapolated these data for all point source inputs to the James as a first
401 approximation of their potential importance to the estuarine C budget. Daily average POC loads
402 from point sources ($0.02 \text{ g m}^{-2} \text{ d}^{-1}$) were too small to appreciably affect our estimate of estuarine
403 POC retention. Point source inputs of DOC ($0.21 \text{ g m}^{-2} \text{ d}^{-1}$) and DIC ($0.36 \text{ g m}^{-2} \text{ d}^{-1}$) were
404 equivalent to 23% and 12% (respectively) of riverine inputs. Taking into account point source
405 contributions, the mass balance suggests that the James tidal fresh segment is a net sink for DOC
406 ($0.12 \text{ g m}^{-2} \text{ d}^{-1}$) and POC ($0.61 \text{ g m}^{-2} \text{ d}^{-1}$) and a net source of DIC ($1.07 \text{ g m}^{-2} \text{ d}^{-1}$). Overall, the
407 James tidal fresh segment was nearly in balance (within 6%) for total C inputs and outputs.

408 Annual average DOC loads to the Pamunkey ($0.67 \pm 0.11 \text{ g m}^{-2} \text{ d}^{-1}$) and Mattaponi (0.89 ± 0.12
409 $\text{g m}^{-2} \text{ d}^{-1}$) were similar to the James ($0.91 \pm 0.12 \text{ g m}^{-2} \text{ d}^{-1}$) on an areal basis. Seasonal variation
410 in DOC inputs followed patterns in discharge with peak values ($0.7 - 1.7 \text{ g m}^{-2} \text{ d}^{-1}$) in winter-
411 spring and minimum values ($0.2 - 0.7 \text{ g m}^{-2} \text{ d}^{-1}$) in summer-fall (Figure 9). Export fluxes closely
412 matched river inputs on a seasonal basis, and balanced to within 10% on an annual basis.
413 Riverine POC inputs to the Pamunkey and Mattaponi (0.17 ± 0.03 and $0.14 \pm 0.02 \text{ g m}^{-2} \text{ d}^{-1}$,
414 respectively) were considerably lower relative to the James ($0.81 \pm 0.15 \text{ g m}^{-2} \text{ d}^{-1}$). For the
415 James, POC inputs were nearly equal to DOC inputs, whereas for the Pamunkey and Mattaponi,
416 DOC accounted for the bulk of OC inputs (79% and 86%, respectively). Export of POC from
417 the Pamunkey and Mattaponi matched inputs to within 10% on an annual basis.

418 3.5 Estuarine Metabolism

419 Rates of GPP and ER were compared to standing stocks (areal values) of DIC and POC to assess
420 the potential influence of C fixation and remineralization on estuarine C concentrations (Figure
421 10). In the James, GPP and ER followed expected seasonal patterns with peak values ($3.5 - 4.0$
422 $\text{g C m}^{-2} \text{ d}^{-1}$) during June-September and low values ($<1 \text{ g C m}^{-2} \text{ d}^{-1}$) in colder months. GPP and
423 ER tracked closely throughout the year, with ER exceeding GPP in colder months, and being
424 equal, or occasionally smaller (June-July) than GPP in warmer months. C fluxes associated with
425 GPP and ER were small in comparison to ambient concentrations of DIC, which ranged from 30
426 to 40 g m^{-2} . By contrast, POC production via GPP was comparable to ambient concentrations of
427 POC, which ranged from 3 g m^{-2} in colder months to 6 g m^{-2} in warmer months. Metabolism of
428 the Pamunkey Estuary was lower and more heterotrophic in comparison to the James. ER varied
429 seasonally from 0.5 to $1.8 \text{ g C m}^{-2} \text{ d}^{-1}$, whereas GPP was persistently low throughout the year ($<$



430 0.5 g C m⁻² d⁻¹). Standing stocks of DIC were large by comparison, ranging from 10 to 40 g m⁻².

431 GPP was small in comparison to standing stocks of POC (3 to 5 g m⁻²).

432 **4.0 Discussion**

433 4.1 C Inputs & Estuarine Concentrations

434 An analysis of C dynamics in the upper portions of the James, Mattaponi and Pamunkey
435 estuaries revealed differences in dominant forms of C and variable responses to changes in river
436 discharge. The James was dominated by products of mineral weathering as DIC accounted for
437 73% of total C with smaller contributions from DOC (20%) and POC (7%). By contrast, organic
438 forms accounted for a larger fraction (49%) of total C in the Pamunkey and Mattaponi. We
439 attribute these differences to variable contributions from local (Coastal Plain) vs. upland
440 (Mountain and Piedmont) runoff. The James Estuary receives inputs from a large catchment
441 with the bulk of runoff (90%) derived from above the Fall Line. By contrast, the Pamunkey and
442 Mattaponi Estuaries receive a greater proportion of their inputs from local tributaries situated
443 within the Coastal Plain. Local floodplains and tidal marshes contribute DOC, while the
444 predominantly sandy soils of the Coastal Plain have low capacity for retaining DOC and
445 contribute little DIC. Differences in source waters may also account for contrasting response in
446 river and estuarine C to high discharge events. We observed larger increases in POC during
447 discharge events in the James, relative to the Pamunkey and Mattaponi. Prior studies
448 documented higher sediment yields from Mountain and Piedmont regions in comparison to the
449 Coastal Plain (Gellis et al. 2009). In source waters to the James, changes in C concentrations
450 with increasing discharge were asynchronous as DIC was negatively related to discharge,
451 whereas POC showed a positive relationship. These findings suggest that DIC export from the
452 watershed is limited by weathering rates (source limited) whereas POC export is transport
453 limited (Wymore et al. 2021). For DIC, this resulted in a dilution response in both the river and
454 estuary, whereas high discharge resulted in a flushing response (enrichment) of POC in the river
455 and estuary. Dilution of estuarine DIC during high discharge was also reported in the nearby
456 Delaware Estuary and linked to reductions in acid neutralizing capacity and greater sensitivity to
457 acidification (Joesef et al. 2017). A strong flushing response was also observed for DOC in the
458 Pamunkey and Mattaponi Rivers, but not the James. Higher DOC concentrations following
459 storm events has been attributed to greater leaching from soils due to higher water elevation and



460 soil inundation (Zarnetske et al. 2018; Patrick et al. 2020). The extensive wetlands and
461 floodplains along the Mattaponi and Pamunkey likely serve as source areas for DOC. Prior work
462 showed that differences in source waters played a role in determining underwater light
463 conditions in these estuaries, as light attenuation in the James was strongly regulated by
464 suspended particulate matter, whereas dissolved organic matter had a greater role in attenuating
465 light in the Pamunkey and Mattaponi estuaries (Henderson and Bukaveckas 2021). Overall, our
466 findings showed strong concentration-discharge relationships in riverine waters, whereas
467 estuarine responses were weaker and more variable. Inter-estuarine differences in C forms and
468 response to discharge were linked to differences in their physiographic setting.

469 4.2 C Mass Balance

470 The tidal freshwater segment of the James Estuary was a net sink for POC and DOC, and a net
471 source of DIC. On an annual basis, external organic matter inputs were attenuated by 28% (± 3)
472 within the tidal fresh segment. Retention of POC accounted for the bulk (84%) of organic matter
473 retention. Peak retention occurred during periods of elevated discharge when inputs of
474 particulate matter to the estuary were highest. The transition from fluvial to tidal conditions
475 favors the settling of suspended particulate matter, which contained ~10-20% organic matter
476 (Bukaveckas et al. 2019). The mass balance indicates that a high proportion (72%) of POC was
477 retained in the tidal fresh segment. Amann et al. (2012) similarly documented high retention of
478 POC in tidal freshwaters of the River Elbe. Our finding is consistent with prior results showing
479 that peak retention of N and P occurred during colder months with elevated river discharge
480 (Bukaveckas and Isenberg 2013). Retention of dissolved N and P was highest during low
481 discharge in summer, but this accounted for a relatively small proportion of total N and P
482 retention on an annual basis. For C, as for N and P, the mass of particulate matter delivered to
483 the estuary during high discharge appears to be the most important determinant of the amount
484 retained within the estuary. Our findings do not support the view that inlands waters function
485 primary as transport systems (“pipes”) during periods of elevated discharge (Zarnetske et al.
486 2018) as the bulk of organic matter retention occurred during high flows in winter, and was
487 associated with the retention of particulates.

488 For the James, atmospheric losses were a small component of the C budget, equivalent to 18% of
489 riverine total C inputs and 15% of total C export. Volta et al. (2016) similarly report that CO₂



490 loss via evasion was ~15% of C export from North Sea estuaries. By contrast, CO₂ evasion from
491 the Pamunkey and Mattaponi was appreciably greater (by 3-fold) relative to the James. Our
492 pCO₂ concentrations for the Pamunkey were similar to those previously reported by Raymond et
493 al. (2000), whereas our air-water flux values were higher (~3 g C m⁻² d⁻¹ vs. ~0.7 g C m⁻² d⁻¹).
494 Comparisons of CO₂ fluxes are complicated by uncertainty regarding atmospheric exchange
495 (Raymond and Cole 2001; Borges et al. 2004; Raymond et al. 2017; Ward et al. 2017).
496 Raymond et al. (2000) used what they considered a conservative exchange coefficient (1.1 m d⁻¹).
497 Substituting their exchange coefficient for the one used in our study yielded similar CO₂ flux
498 values. More recent studies have adopted higher exchange coefficients, particularly for systems
499 where tidal and fluvial forces likely play a greater role in determining boundary layer conditions
500 than are predicted from wind-based models.

501 Tidal fluxes were not a large component of the mass balance for any of the C fractions.
502 Although the volume of water exchanged during a tidal cycle was large (tidal prism = 28% of
503 estuarine volume), the elongate shape of the estuary dictates that water leaving on an out-going
504 tide returns on the subsequent in-coming tide. Results from the C_I mass balance suggest that the
505 net tidal exchange was ~7% of the tidal prism, equivalent to 2% of estuarine volume. In
506 addition, we observed weak C gradients across the lower boundary of the study reach indicating
507 that tidal inputs and outputs largely offset.

508 4.3 Metabolism & Carbon

509 Mass balance and metabolism data provide independent evidence that these estuaries are net
510 heterotrophic. The mass balance indicates that the James is a sink for organic C and a source of
511 inorganic C, consistent with metabolism data showing that ecosystem respiration exceeds GPP.
512 Greater heterotrophy was observed in the Pamunkey where respiration rates were comparable to
513 the James, but GPP was substantially lower. This finding was consistent with the observed
514 higher CO₂ concentrations and efflux. The evasion of CO₂ from the Pamunkey and Mattaponi
515 was large (3x) in comparison to riverine inputs of DOC and POC, whereas CO₂ loss from the
516 James was ~50% of riverine OM inputs. We attribute the greater heterotrophy of the former to
517 differences in hydrogeomorphology and forms of primary production. Higher chlorophyll-a
518 values in the James indicate greater phytoplankton contributions to GPP, which brings the tidal
519 fresh segment more closely in balance with respect to production and respiration. The



520 Pamunkey and Mattaponi have low chlorophyll-a by comparison (Bukaveckas et al. 2020) but
521 extensive lateral floodplains and emergent marshes (Hupp et al. 2009; Noe and Hupp 2009; Lake
522 et al. 2013). Decomposition of terrestrial organic matter during floodplain inundation may
523 account for the high CO₂ concentrations and air-water fluxes during high discharge conditions.
524 Van Dam et al. (2018) similarly reported that high CO₂ losses during flooding events accounted
525 for 30-40% of annual emissions from North Carolina estuaries. An accounting of changes in
526 floodplain C stores before and after inundation events is needed to better understand their role in
527 supporting respiration in these systems. Organic matter inputs following senescence of emergent
528 vegetation may also contribute to higher rates of respiration and CO₂ evasion. Emergent plant
529 production would not be captured in our diel dissolved-O₂ based estimates of ecosystem GPP,
530 which may over-estimate heterotrophy in this system. Overall, our results based on C mass
531 balance and ecosystem metabolism approaches suggest that the upper segments of these estuaries
532 are net heterotrophic. This finding is consistent with a meta-analysis of metabolism data
533 showing that estuaries are generally net heterotrophic (Hoellein et al. 2013), but contrasts with
534 recent work by Brodeur et al. (2019) showing that the Susquehanna River and mainstem
535 Chesapeake Bay are a net sink for DIC, and therefore net autotrophic.

536 Despite the large riverine influence in these upper estuarine segments, internal cycling of C via
537 production and respiration was large in comparison to external forcing via fluvial and tidal
538 exchange (Figure 11). In summer, remineralization of C via respiration was almost 2-fold
539 greater in comparison to external DIC inputs. In winter, the balance tipped strongly in favor of
540 external inputs as riverine DIC contributions were 3-fold greater than internal production via
541 respiration. Internal production of POC via GPP was an order of magnitude higher than external
542 inputs of POC in summer. In winter, GPP contributions were approximately equal to external
543 inputs of POC. Based on GPP, the estimated turnover time of the POC pool was 1.5 d in
544 summer. Taking into account that 60% of POC in the James is algal (Wood et al. 2016), the
545 estimated phytoplankton turnover time was 0.9 d. The high rates of internal biological
546 processing relative to through-puts of C places the James toward the lake-end, rather than the
547 stream-river end, on the metabolism and residence time spectrum (Hotchkiss et al. 2018). This is
548 likely a consequence of tidal conditions, which allow for longer water residence compared to
549 non-tidal rivers. Proximal nutrient inputs (from riverine and point sources) and poor water
550 clarity (due to suspended sediments), likely also contribute to the dominance of phytoplankton



551 over aquatic plants in this system. If recent increases in water clarity continue (Henderson and
552 Bukaveckas 2021), we would expect a shift toward macrophyte dominance, lower GPP:ER, and
553 a diminished influence of internal C cycling.

554 The tidal fresh segment of the James has moderately low DIC and high GPP, which raises the
555 question whether primary production is limited by the availability of inorganic C. Our data show
556 that daily autotrophic C demand is small (~10%) relative to the available DIC pool. In summer,
557 DIC requirements to sustain GPP exceed the rate of external supply via river inputs, but
558 remineralization of C via respiration is approximately equal to GPP, indicating that internal
559 cycling is sufficiently large to preclude C limitation. However, a case could be made for
560 potential C limitation of photosynthesis due to depletion of pCO₂. The diffusion of CO₂ in water
561 occurs more slowly than in air, potentially resulting in depletion during periods of high
562 autotrophic demand. In the James, low CO₂, with occasional under-saturation, was observed in
563 summer at stations corresponding to the CHL_a maximum. Other studies in riverine settings have
564 shown that phytoplankton can reduce CO₂ to near or below atmospheric equilibrium (Raymond
565 et al. 1997; Crawford et al. 2017). As CO₂ is energetically favored for carbon fixation, depletion
566 of CO₂ may reduce production efficiency and alter community structure by favoring taxa capable
567 of using bicarbonates. A number of prior studies have linked primary production and pCO₂
568 (Jansson et al. 2012; Low-Decarie et al. 2015; Hasler et al. 2016). Our CO₂ data were collected
569 mid-morning, closer to the diel maximum than the afternoon minimum (Crosswell et al. 2017;
570 Reiman and Xu 2019), thereby potentially under-estimating CO₂ depletion. We cannot discount
571 the possibility that phytoplankton-driven CO₂ depletion in the James may affect production and
572 community composition, though this effect appears limited to mid-summer and stations located
573 at the CHL_a maximum.

574 4.4 C Sources & Consumer Energetics

575 Lastly, we consider the utility of our C mass balance for understanding trophic energetics of the
576 James food web, particularly with respect to autochthony and allochthony. There are advantages
577 to combining mass balance, ecosystem metabolism and bioenergetics approaches, though there
578 are few examples, often, as in this case, due to a lack of data on consumer production (Ruegg et
579 al. 2021). From a mass flux perspective, a comparison of autochthonous (GPP = 719 ± 32 g C
580 m⁻² y⁻¹) and allochthonous (POC = 298 ± 56, DOC = 340 ± 44 g C m⁻² y⁻¹) inputs suggests that



581 internal C sources are nearly equal ($54 \pm 4\%$) to external inputs, despite the large riverine
582 influence in the upper estuary. We can refine these estimates to better reflect availability for
583 consumers by discounting GPP by 40% to reflect loss via autotrophic respiration (Ruegg et al.
584 2021) and taking into account the fraction POC and DOC that is retained ($28 \pm 3\%$). By this
585 estimate, autochthonous production contributes 70% ($431 \text{ g C m}^{-2} \text{ y}^{-1}$) and allochthonous inputs
586 30% ($203 \text{ g C m}^{-2} \text{ y}^{-1}$) of C available to consumers. These percentages are based on annualized
587 values though their relative importance varies seasonally with the majority of GPP occurring in
588 May to October, and the bulk of POC delivered in January to May.

589 Comparisons of mass fluxes may not be indicative of C supporting secondary production if
590 consumers preferentially utilize one source over another. A number of studies have suggested
591 that autochthonous sources account for a disproportionately large fraction of C assimilation due
592 to the higher nutritional quality of algae over partially decomposed terrestrial plant matter (Brett
593 et al. 2009; Thorp and Bowes 2017). Stable isotope analysis of the James food web has shown
594 that the dominant metazoans by biomass, which are benthic omnivores (catfish, adult gizzard
595 shad), carry a predominantly terrestrial C signature, whereas zooplankton and planktivorous fish
596 (juvenile gizzard shad and threadfin shad) were dependent on autochthonous C sources (Wood et
597 al. 2016). These patterns were consistent with analysis of basal resources showing that the
598 sediments in the estuary were largely (90%) comprised of terrestrial C, whereas seston contained
599 a greater fraction of autochthonous C (60% in summer).

600 The lack of secondary production data does not allow us to align C supply from autochthonous
601 and allochthonous sources with C demands of consumers. However, the rate of biomass removal
602 for one of the dominant metazoans (catfish) can be used as a first approximation of their annual
603 production. Catfish were introduced to the James during the 1970's and 1980's and now
604 dominate the fishery (Fabrizio et al. 2018), which has led to questions about their influence on
605 food webs and ecosystem processes (Greenlee and Lim 2011; Hilling et al. 2019; Schmitt et al.
606 2019). The biomass of catfish removed from the James represents a conservative estimate of
607 their annual production in that current harvest rates have not brought about declines in the catfish
608 population, indicating that annual production exceeds the amount of biomass removed (Orth et
609 al. 2017). During 2010-2020, the commercial harvest of catfish in the tidal James averaged
610 1,000,000 lbs y^{-1} (data provided by Virginia Marine Resources Commission), which taking into



611 account the area of the fresh-brackish estuary, yields a harvest rate of $8.6 \text{ kg ha}^{-1} \text{ y}^{-1}$. In addition
612 to the commercial harvest, piscivorous birds are an important component of biomass removal.
613 Here we focus on predation by bald eagles and osprey as there are census data during the
614 breeding season (from areal surveys) and estimates of catfish contributions to adult and nestling
615 diets (from direct observations and stable isotopes; Garman et al. 2010). Based on census data
616 and bioenergetics modeling, fish consumption by bald eagles and osprey was estimated at 0.6 kg
617 $\text{ha}^{-1} \text{ d}^{-1}$ for the James tidal fresh segment. Taking into account the contribution of catfish to the
618 diet of bald eagles and osprey ($\sim 35\%$) yields an estimate of catfish biomass removal of 77 kg ha^{-1}
619 y^{-1} , which is ~ 9 -fold higher than for commercial fisheries. With further corrections for the
620 moisture content (75%; Cresson et al. 2017) and C content of fish tissues (45%; Tanner et al.
621 2000), the total catfish removal by birds and commercial fishing is $0.96 \text{ g C m}^{-2} \text{ y}^{-1}$. Their
622 trophic position in the James (trophic level = 3.1; Orth et al. 2017) suggests a production
623 efficiency of $\sim 1\%$ (Ruegg et al. 2021), which yields an estimated C demand to maintain this
624 level of production/harvest of $96 \text{ g C m}^{-2} \text{ y}^{-1}$. The C demand for this introduced species
625 corresponds to 15% of C available to consumers from allochthonous and autochthonous sources.
626 Stable isotope data indicate that catfish in the James tidal fresh obtain 9% of their C from
627 autochthonous sources and 81% from allochthonous sources (Wood et al. 2016). Applying these
628 values suggests that 2% of GPP and 41% of allochthonous inputs are required to sustain current
629 levels of catfish biomass removal from the James tidal fresh. The high rate of utilization for
630 allochthonous inputs is consistent with our prior finding that consumer-mediated recycling is an
631 important component of nutrient supply, and may account for the lack of response in primary
632 production to large reductions in point source nutrient inputs (Wood et al. 2014).

633 4.5 Summary

634 Relatively complete C budgets are relatively rare, in part due to the effort involved in quantifying
635 C fluxes from various sources (Hanson et al. 2015). This paper provides an accounting of major
636 C fluxes into and out of the upper segments of the James, Pamunkey and Mattaponi Estuaries.
637 The C budget for the tidal freshwater segment of the James is fairly robust in that it includes tidal
638 exchange, point sources and internal transformations via production and respiration over a span
639 of years and discharge conditions. The findings show that the relative importance of external
640 (river inputs & tidal exchange) vs. internal (metabolism) drivers differed among the three



641 estuaries based on their physiographic setting and forms of primary production. Estuarine C
642 forms were influenced by variable contributions from upland (DIC-rich, POC-rich) and lowland
643 (DOC-rich) sources. Peak organic matter retention was associated with trapping of POC during
644 high discharge conditions. Tidal exchange was not an important component of the C budget,
645 whereas biological transformations via production and respiration were large in the
646 phytoplankton-dominated James Estuary. Contrary to expectations, autochthonous sources
647 accounted for the bulk of organic matter inputs despite the large riverine influence on the upper
648 estuary. Commercial harvest data and previously derived estimates of piscivory by birds
649 provided a basis for estimating consumer C demand, albeit for a single dominant species, and at
650 a coarse (annualized) scale. Further progress in aligning C flows to food web energetics depends
651 on the availability of production data for a greater range of consumers and at shorter time
652 intervals. Bringing together C mass balance, ecosystem metabolism and consumer production
653 data would enable a potentially powerful approach for advancing our understanding of how the
654 timing and sources of C inputs constrain trophic energetics.

655

656 Acknowledgements

657 Thanks to Samantha Rogers who drafted figures for this paper, to D. Hopler, S. Tassone and W.
658 M. Lee who carried out the field and lab work, and to Donald Orth for helpful discussions
659 regarding catfish in the James. I am grateful to the USGS for providing discharge, DOC and
660 POC data for Fall Line stations and to the Virginia Institute of Marine Science for making
661 available dissolved oxygen data from the Pamunkey.

662 Data availability

663 Data can be accessed upon request to the corresponding author.

664 Competing interests

665 The author declares that there is no conflict of interest.

666



667 Reference List

- 668
669 Alin, S. R., F. L. de Fatima, M. Rasera, C. I. Salimon, J. E. Richey, G. W. Holtgrieve, A. V.
670 Krusche, and A. Snidvongs 2011. Physical controls on carbon dioxide transfer velocity
671 and flux in low-gradient river systems and implications for regional carbon budgets.
672 *Journal of Geophysical Research: Biogeosciences* 116: G01009.
- 673 Amann, T., A. Weiss, and J. Hartmann. 2012. Carbon dynamics in the freshwater part of the
674 Elebe estuary, Germany: Implications of improving water quality. *Estuarine, Coastal and*
675 *Shelf Science* 107: 112-121.
- 676 Amann, T., A. Weiss, and J. Hartmann. 2015. Inorganic carbon fluxes in the inner Elbe Estuary,
677 Germany. *Estuaries and Coasts* 38: 192-210.
- 678 Basu, B. K., and F. R. Pick 1996. Factors regulating phytoplankton and zooplankton biomass in
679 temperate rivers. *Limnology and Oceanography* 41: 1572-1577.
- 680 Bianchi, T. S. 2011. The role of terrestrially derived organic carbon in the coastal ocean: a
681 changing paradigm and the priming effect. *Proceedings of the National Academy of*
682 *Sciences USA* 108: 19473-19481.
- 683 Borges, A. V., B. Delille, L.-S. Schiettecatte, F. Gazeau, G. Abril, and M. Frankignoulle 2004.
684 Gas transfer velocities of CO₂ in three European estuaries (Randers Fjord, Scheldt, and
685 Thames). *Limnology and Oceanography* 49: 1630-1641.
- 686 Brett, M. T., M. Kainz, S. Taipale, and H. Seshan 2009. Phytoplankton, not allochthonous
687 carbon, sustains herbivorous zooplankton production. *Proceedings of the National*
688 *Academy of Sciences USA* 106: 21197-21201.
- 689 Brodeur, J. R., B. Chen, J. Su, Y.-Y. Xu, N. Hussain, K. M. Scaboo, Y. Zhang, J. M. Testa, and
690 W.-J. Cai 2019. Chesapeake Bay inorganic carbon: distribution and seasonal variability.
691 *Frontiers in Marine Science* 6: 99.
- 692 Bukaveckas, P. A., L. E. Barry, M. J. Beckwith, V. David, and B. Lederer 2011. Factors
693 determining the location of the chlorophyll maximum and the fate of algal production
694 within the tidal freshwater James River. *Estuaries and Coasts* 34: 569-582.
- 695 Bukaveckas, P. A., and W. N. Isenberg. 2013. Loading, transformation and retention of nitrogen
696 and phosphorus in the tidal freshwater James River (Virginia). *Estuaries and Coasts* 36:
697 1219-1236.
- 698 Bukaveckas, P. A., and J. D. Wood 2014. Nitrogen retention in a restored tidal stream (Kimages
699 Creek, VA) assessed by mass balance and tracer approaches. *Journal of Environmental*
700 *Quality* 43: 1614-1623.
- 701 Bukaveckas, P. A., M. Beck, D. Devore, and W. M. Lee 2018. Climate variability and its role in
702 regulating C, N and P retention in the James River Estuary. *Estuarine, Coastal and Shelf*
703 *Science* 205: 161-173.
- 704 Bukaveckas, P. A., M. Katarzyte, A. Schlegel, R. Spuriene, T. A. Egerton, and D. Vaiciute 2019.
705 Composition and settling properties of suspended particulate matter in estuaries of the
706 Chesapeake Bay and Baltic Sea regions. *Journal of Soils and Sediments* 19: 2580-2593.



- 707 Bukaveckas, P. A., S. Tassone, W. M. Lee, and R. B. Franklin 2020. The influence of storm
708 events on metabolism and water quality of riverine and estuarine segments of the James,
709 Mattaponi and Pamunkey Rivers. *Estuaries and Coasts* 43: 1585-1602.
- 710 Butman, D., S. Stackpoole, E. G. Stets, C. P. McDonald, D. W. Clow, and R. G. Striegl 2016.
711 Aquatic carbon cycling in the conterminous United States and implications for terrestrial
712 carbon accounting. *Proceedings of the National Academy of Sciences USA* 113: 58-63.
- 713 Caffrey, J. M. 2003. Production, respiration and net ecosystem metabolism in U.S. estuaries.
714 *Environmental Monitoring and Assessment* 81: 207-219.
- 715 Caffrey, J. M. 2004. Factors controlling net ecosystem metabolism in U.S. estuaries. *Estuaries*
716 27: 90-101.
- 717 Cai, W.-J., and Y. Wang 1998. The chemistry, fluxes and sources of carbon dioxide in the
718 estuarine waters of the Satilla and Altamaha Rivers, Georgia. *Limnology and*
719 *Oceanography* 43: 657-668.
- 720 Cole, J. J., Y. T. Prairie, N. F. Caraco, W. H. McDowell, L. J. Tranvik, R. G. Striegl, C. M.
721 Duarte, P. Kortelainen, J. A. Downing, J. J. Middelburg, and J. M. Melack 2007.
722 Plumbing the global carbon cycle: integrating inland waters into the terrestrial carbon
723 budget. *Ecosystems* 10: 171-184.
- 724 Crawford, J. T., D. Butman, L. C. Loken, P. Stadler, C. Kuhn, and R. G. Striegl 2017. Spatial
725 variability of CO₂ concentrations and biogeochemistry in the Lower Columbia River.
726 *Inland Waters* 7: 417-427.
- 727 Cresson, P., M. Travers-Trolet, M. Rouquette, C-A. Timmerman, C. Giraldo, S. Lefebvre, and B.
728 Ernande. 2017. Underestimation of chemical contamination in marine fish muscle tissue
729 can be reduced by considering variable wet:dry weight ratios. *Marine Pollution Bulletin*.
730 123: 279-285.
- 731 Crosswell, J. R., I. C. Anderson, J. W. Stanhope, B. Van Dam, M. J. Brush, S. H. Ensign, M. F.
732 Piehler, B. McKee, M. Bost, and H. W. Paerl 2017. Carbon budget of a shallow lagoonal
733 estuary: transformations and source-sink dynamics along the river-estuary-ocean
734 continuum. *Limnology and Oceanography* 62: S29-S45.
- 735 Fabrizio, M. C., T. D. Tuckey, R. J. Latour, G. C. White, and A. J. Norris 2018. Tidal habitats
736 support large numbers of invasive blue catfish in a Chesapeake Bay sub-estuary.
737 *Estuaries and Coasts* 41: 827-840.
- 738 Garman, G., C. Viverette, B. Watts, and S. Macko. 2010. Predator-prey Interactions among
739 Fish-eating Birds and selected Fishery Resources in the Chesapeake Bay: Temporal and
740 Spatial Trends and Implications for Fishery Assessment and Management. William &
741 Mary Center for Conservation Biology Technical Report #349.
742 https://scholarworks.wm.edu/ccb_reports/349.
- 743 Gellis, A.C. and others. 2009. Sources, transport, and storage of sediment in the Chesapeake
744 Bay Watershed. U.S. Geological Survey Scientific Investigations Report 2008–5186.
- 745 Greenlee, R. S., and C. N. Lim 2011. Searching for equilibrium: population parameters and
746 variable recruitment in introduced blue catfish populations in four Virginia tidal river
747 systems. *American Fisheries Society Symposium* 77: 349-367.



- 748 Hanson, P. C., M. L. Pace, S. R. Carpenter, J. J. Cole, and E. H. Stanley 2015. Integrating
749 landscape carbon cycling: research needs for resolving organic carbon budgets of lakes.
750 *Ecosystems* 18: 363-375.
- 751 Hasler, C. T., D. Butman, J. D. Jeffrey, and C. D. Suski 2016. Freshwater biota and rising pCO₂?
752 *Ecology Letters* 19: 98-108.
- 753 Henderson, R. and P.A. Bukaveckas. 2021. Factors governing light attenuation in upper
754 segments of the James and York Estuaries and their influence on primary producers.
755 *Estuaries & Coasts* <https://doi.org/10.1007/s12237-021-00983-6>.
- 756 Hilling, C. D., A. J. Bunch, J. A. Emmel, J. D. Schmitt, and D. J. Orth 2019. Growth and
757 mortality of invasive flathead catfish in the tidal James River, Virginia. *Journal of Fish
758 and Wildlife Management* 10: 641-652.
- 759 Hoellein, T. J., D. A. Bruesewitz, and D. C. Richardson 2013. Revisiting Odum (1956): a
760 synthesis of aquatic ecosystem metabolism. *Limnology and Oceanography* 58: 2089-
761 2100.
- 762 Hoffman, J. C., D. A. Bronk, and J. E. Olney 2008. Organic matter sources supporting lower
763 food web production in the tidal freshwater portion of the York River estuary. *Estuaries
764 and Coasts* 31: 898-911.
- 765 Hotchkiss, E. R., S. Sadro, and P. C. Hanson 2018. Toward a more integrative perspective on
766 carbon metabolism across lentic and lotic inland waters. *Limnology and Oceanography:
767 Letters* 3: 57-63.
- 768 Hoitink, A. J. F., and D. A. Jay 2016. Tidal river dynamics: implications for deltas. *Reviews of
769 Geophysics* 54: 240-272.
- 770 Holgerson, M. A., and P. A. Raymond 2016. Large contribution to inland water CO₂ and CH₄
771 emissions from very small ponds. *Nature Geoscience* doi: 10.1038/ngeo2654.
- 772 Hupp, C. R., A. R. Pierce, and G. B. Noe 2009. Floodplain geomorphic processes and
773 environmental impacts of human alteration along Coastal Plain rivers, USA. *Wetlands
774* 29: 413-429.
- 775 Jansson, M., J. Karlsson, and A. Jonsson 2012. Carbon dioxide super-saturation promotes
776 primary production in lakes. *Ecology Letters* 15: 527-532.
- 777 Joesoef, A., D. L. Kirchman, C. K. Sommerfield, and W.-J. Cai 2017. Seasonal variability of the
778 inorganic carbon system in a large coastal plain estuary. *Biogeosciences* 14: 4949-4963.
- 779 Jones, A. E., A. K. Hardison, B. R. Hodges, J. W. McClelland, and K. B. Moffett 2020. Defining
780 a riverine tidal freshwater zone and its spatiotemporal dynamics. *Water Resources
781 Research* 56: e2019WRR026619.
- 782 Lake, S.J., M.J. Brush, I.C. Anderson, and H.I. Kator. 2013. Internal versus external drivers of
783 periodic hypoxia in a coastal plain tributary estuary: the York River, Virginia. *Marine
784 Ecology Progress Series* 492: 21-39.
- 785 Lionard, M., K. Muylaert, A. Hanoutti, T. Maris, M. Tackx, and W. Vyverman 2008. Inter-
786 annual variability in phytoplankton summer blooms in the freshwater tidal reaches of the
787 Schelde estuary (Belgium). *Estuarine, Coastal and Shelf Science* 79: 694-700.



- 788 Low-Decarie, E., G. Bell, and G. F. Fussman 2015. CO₂ alters community composition and
789 response to nutrient enrichment of freshwater phytoplankton. *Oecologia* 177: 875-883.
- 790 Lucas, L. V., J. K. Thompson, and L. R. Brown 2009. Why are diverse relationships observed
791 between phytoplankton biomass and transport time? *Limnology and Oceanography* 54:
792 381-390.
- 793 Meybeck, M. 2003. Global analyses of river systems: from Earth system controls to
794 Anthropocene syndromes. *Phil. Trans. R. Soc. Lond. B* 358: 1935-1955.
- 795 Middelburg, J. J., and P. M. J. Herman 2007. Organic matter processing in tidal estuaries. *Marine*
796 *Chemistry* 106: 127-147.
- 797 Morton, R., and B. L. Henderson 2008. Estimation of non-linear trends in water quality: an
798 improved approach using generalized additive models. *Water Resources Research* 44:
799 W07420.
- 800 Murphy, R. R., E. Perry, J. Harcum, and J. Keisman 2019. A Generalized Additive Model
801 approach to evaluating water quality: Chesapeake Bay case study. *Environmental*
802 *Modelling and Software* 118: 1-13.
- 803 Muylaert, K., M. Tackx, and W. Vyverman 2005. Phytoplankton growth rates in the tidal
804 freshwater reaches of the Schelde estuary (Belgium) estimated using a simple light-
805 limited primary production model. *Hydrobiologia* 540: 127-140.
- 806 Noe, G. B., and C. R. Hupp 2009. Retention of riverine sediment and nutrient loads by Coastal
807 Plain floodplains. *Ecosystems* 12: 728-746.
- 808 Orth, D.J., Y. Jiao, J.D. Schmidt, C.D. Hilling, J.A. Emmel and M.C. Fabrizio. 2017. Dynamics
809 and Role of Non-native Blue Catfish *Ictalurus furcatus* in Virginia's Tidal Waters. Final
810 Report submitted to Virginia Department of Game and Inland Fisheries. DOI:
811 10.13140/RG.2.2.35917.54246.
- 812 Pace, M. L., S. E. G. Findlay, and D. Lints 1992. Zooplankton in advective environments: the
813 Hudson River community and a comparative analyses. *Canadian Journal of Fisheries and*
814 *Aquatic Sciences* 49: 1060-1069.
- 815 Patrick, C. J., and others 2020. A system level analysis of coastal ecosystem responses to
816 hurricane impacts. *Estuaries and Coasts* 43: 943-959.
- 817 Qin, Q., and J. Shen 2017. The contribution of local and transport processes to phytoplankton
818 biomass variability over different time scales in the Upper James River, Virginia.
819 *Estuarine, Coastal and Shelf Science* 196: 123-133.
- 820 Raymond, P. A., J. E. Bauer, and J. J. Cole 2000. Atmospheric CO₂ evasion, dissolved inorganic
821 carbon production, and net heterotrophy in the York River estuary. *Limnology and*
822 *Oceanography* 45: 1707-1717.
- 823 Raymond, P. A., N. F. Caraco, and J. J. Cole 1997. Carbon dioxide concentration and
824 atmospheric flux in the Hudson River. *Estuaries* 20: 381-390.
- 825 Raymond, P. A., and J. J. Cole 2001. Gas exchange in rivers and estuaries: Choosing a gas
826 transfer velocity. *Estuaries* 24: 312-317.



- 827 Raymond, P. A., J. Hartmann, R. Lauerwald, S. Sobek, C. P. McDonald, M. Hoover, D. Butman,
828 R. G. Striegl, E. Mayorga, C. Humborg, P. Kortelainen, H. Durr, M. Meybeck, P. Ciais,
829 and P. Guth 2017. Global carbon dioxide emissions from inland waters. *Nature* 503: 355-
830 359.
- 831 Reiman, J. H., and Y. J. Xu 2019. Diel variability of PCO₂ and CO₂ outgassing from the lower
832 Mississippi River: implications for riverine CO₂ outgassing estimation. *Water* 11: 43.
- 833 Richey, J. E., J. M. Melack, A. Aufdenkampe, V. M. Ballester, and L. L. Hess 2002. Outgassing
834 from Amazonian rivers and wetlands as a large tropical source of atmospheric CO₂.
835 *Nature* 416: 617-620.
- 836 Robson, B. J., P. A. Bukaveckas, and D. P. Hamilton 2008. Modelling and mass balance
837 assessments of nutrient retention in a seasonally-flowing estuary (Swan River Estuary,
838 Western Australia). *Estuarine, Coastal and Shelf Science* 76: 282-292.
- 839 Ruegg, J., C. C. Conn, E. P. Anderson, T. J. Battin, E. S. Bernhardt, M. B. Canadell, S. M.
840 Bonjour, J. D. Hosen, N. S. Marzolf, and C. B. Yackulic 2021. Thinking like a consumer:
841 linking aquatic basal metabolism and consumer dynamics. *Limnology and*
842 *Oceanography: Letters* 6: 1-17.
- 843 Schmitt, J. D., B. K. Peoples, L. Castello, and D. J. Orth 2019. Feeding ecology of generalist
844 consumers: a case study of invasive blue catfish *Ictalurus furcatus* in Chesapeake Bay,
845 Virginia, USA. *Environmental Biology of Fishes* 102: 443-465.
- 846 Sellers, T., and P. A. Bukaveckas 2003. Phytoplankton production in a large, regulated river: A
847 modeling and mass balance assessment. *Limnology and Oceanography* 48: 1476-1487.
- 848 Shen, J., and J. Lin 2006. Modeling study of the influences of tide and stratification on age of
849 water in the tidal James River. *Estuarine, Coastal and Shelf Science* 68: 101-112.
- 850 Soballe, D. M., and B. L. Kimmel 1987. A large-scale comparison of factors influencing
851 phytoplankton abundance in rivers, lakes, and impoundments. *Ecology* 68: 1943-1954.
- 852 Steen, A.D., L. M. Quigley and A. Buchan. 2015. Evidence for the priming effect in a
853 planktonic estuarine microbial community. *Frontiers in Marine Science* 3:6.
854 doi:10.3389/fmars.2016.00006.
- 855 Tassone, S., and P. A. Bukaveckas 2019. Seasonal, interannual and longitudinal patterns in
856 estuarine metabolism derived from diel oxygen data using multiple computational
857 approaches. *Estuaries and Coasts* 42: 1032-1051.
- 858 Thorp, J. H., and R. E. Bowes 2017. Carbon sources in riverine food webs: new evidence from
859 amino acid isotope techniques. *Ecosystems* 20: 1029-1041.
- 860 Tranvik, L. J., J. A. Downing, J. B. Cotner, and others 2009. Lakes and reservoirs as regulators
861 of carbon cycling and climate. *Limnology and Oceanography* 54: 2298-2314.
- 862 Tranvik, L. J., J. J. Cole, and Y. T. Prairie 2018. The study of carbon in inland waters - from
863 isolated ecosystems to players in the global carbon cycle. *Limnology and Oceanography:*
864 *Letters* 3: 41-48.



- 865 Van Dam, B. R., J. R. Crosswell, and H. W. Paerl 2018. Flood-driven CO₂ emissions from
866 adjacent North Carolina estuaries during Hurricane Joaquin (2015). *Marine Chemistry*
867 207: 1-12.
- 868 Vincent, W. F., J. J. Dodson, N. Bertrand, and J.-J. Frenette 1996. Photosynthetic and bacterial
869 production gradients in a larval fish nursery: The St. Lawrence River transition zone.
870 *Marine Ecology Progress Series* 139: 227-238.
- 871 Volta, C., G. G. Laruelle, and P. Regnier 2016. Regional carbon and CO₂ budgets of North Sea
872 tidal estuaries. *Estuarine, Coastal and Shelf Science* 176: 76-90.
- 873 Vorosmarty, C. J., M. Meybeck, B. M. Fekete, K. P. Sharma, P. Green, and J. P. M. Syvitski
874 2003. Anthropogenic sediment retention: major global impact from registered river
875 impoundments. *Global and Planetary Change* 39: 169-190.
- 876 Ward, N. D. and others. 2016. The reactivity of plant-derived organic matter and the potential
877 importance of priming effects in the lower Amazon River. *JGR-Biogeosciences* 121:
878 1522–1539.
- 879 Ward, N. D., T. S. Bianchi, P. M. Medeiros, M. Seidel, J. E. Richey, R. G. Keil, and H. O.
880 Sawakuchi 2017. Where carbon goes when water flows: carbon cycling across the
881 aquatic continuum. *Frontiers in Marine Science* 4: 7.
- 882 Wiik, E., H. A. Haig, N. M. Hayes, K. Finlay, G. L. Simpson, R. J. Vogt, and P. R. Leavitt 2021.
883 Generalized additive models of climatic and metabolic controls of subannual variation in
884 pCO₂ in productive hardwater lakes. *Journal of Geophysical Research: Biogeosciences*
885 123: 1940-1959.
- 886 Wood, J. D., and P. A. Bukaveckas 2014. Increasing severity of phytoplankton nutrient
887 limitation following reductions in point source inputs to the tidal freshwater segment of
888 the James River Estuary. *Estuaries and Coasts* 37: 1188-1201.
- 889 Wood, J. D., D. Elliott, G. C. Garman, D. Hopler, W. Lee, S. McIninch, A. J. Porter, and P. A.
890 Bukaveckas 2016. Autochthony, allochthony and the role of consumers in influencing the
891 sensitivity of aquatic systems to nutrient enrichment. *Food Webs* 7: 1-12.
- 892 Wood, S., 2006. *Generalized Additive Models: an Introduction with R*, 1 ed. Chapman and
893 Hall/CRC, Boca Raton, FL.
- 894 Wymore, A. S., H. M. Fazekas, and W. H. McDowell 2021. Quantifying the frequency of
895 synchronous carbon and nitrogen export to the river network. *Biogeochemistry* 152: 1-12.
- 896 Yang, G., and D. L. Moyer 2020. Estimation of non-linear water quality trends in high-frequency
897 monitoring data. *Science of the Total Environment* 715: 136686.
- 898 Young, M., E. Hoew, T. O'Rear, K. Berridge, and P. Moyle 2021. Food web fuel differs across
899 habitats and seasons of a tidal freshwater estuary. *Estuaries and Coasts* 44: 286-301.
- 900 Zarnetske, J. P., M. Bouda, B. W. Abbott, J. Saiers, and P. A. Raymond 2018. Generality of
901 hydrologic transport limitation of watershed organic carbon flux across ecoregions of the
902 United States. *Geophysical Research Letters* 45: 11702-11711.



903 Table 1. Data collection sites for this study include USGS Fall Line gauging stations (Q denotes
904 discharge), estuarine sampling sites and an ungauged Coastal Plain tributary of the James
905 (Kimages Creek). Station numbers denote distance in river miles from the confluence with
906 Chesapeake Bay (James) or the York (Pamunkey and Mattaponi). Observations denote the
907 number of sampling dates for water chemistry within the specified time span.

Tributary	Segment	Stations	Parameters	Years	Observations	Source
James	River	JMS110	Q, DOC, POC	2010-19	197	USGS (02037500)
		JMS110	Cl, DIC, pCO ₂	2012-19	189	This Study
	Estuary	JMS99,75,69,56	Cl, DOC, POC, DIC, pCO ₂	2015-19	105	This Study
	Ungauged	Kimages Creek	Cl, DOC, POC, DIC, pCO ₂	2012-19	211	This Study
Pamunkey	River	PMK82	Q, DOC, POC	2010-19	202	USGS (01673000)
	Estuary	PMK50,39,6	DOC, POC, DIC, pCO ₂	2017-19	60	This Study
Mattaponi	River	MPN54	Q, DOC, POC	2010-19	203	USGS (01674500)
	Estuary	MPN36,29,4	DOC, POC, DIC, pCO ₂	2017-19	60	This Study

908

909



910 Table 2. GAM analysis of seasonal (day of year; DOY), inter-annual (date) and discharge
 911 dependent variation in river, tributary and estuarine DOC, POC, DIC, pCO₂ and Cl. Data are for
 912 riverine and upper estuarine segments of the James, Mattaponi and Pamunkey as well as a local
 913 (below Fall Line) tributary (Kimages Creek). Statistics include the adjusted R², root mean
 914 square error (RMSE as mg L⁻¹, except pCO₂ = ppmv), and significance of s values with their
 915 effective degrees of freedom (** denotes p < 0.001; * p < 0.05).

916

Model	Fraction	Site	Adj R ²	RMSE	s(DOY)	s(date)	s(discharge)
River	DOC	James	0.50	0.82	3.42**	8.52**	3.00**
		Mattaponi	0.81	1.00	5.66**	8.93**	5.43**
		Pamunkey	0.67	1.06	4.64**	8.61**	5.54**
	POC	James	0.76	1.74	3.67**	7.89**	8.20**
		Mattaponi	0.38	0.61	3.99**	6.34	6.25**
		Pamunkey	0.51	1.08	2.39**	8.95**	7.79**
	DIC	James	0.44	4.19	2.42**	7.89**	8.20**
pCO ₂	James	0.67	149	3.37**	6.43**	3.59**	
Cl	James	0.48	4.36	7.23**	8.30**	6.73**	
Tributary	DOC	Kimages	0.33	3.22	4.70**	8.26**	NA
	POC	Kimages	0.24	0.57	4.61**	7.63**	NA
	DIC	Kimages	0.19	3.00	0.41	8.26**	NA
	Cl	Kimages	0.23	8.63	6.46**	6.48**	NA
Estuary	DOC	James	0.13	3.44	4.29	1.96	1.91*
		Mattaponi	0.27	2.37	5.65	3.42**	1.00
		Pamunkey	0.27	2.61	5.94*	3.95**	1.00
	POC	James	0.75	0.22	5.77**	2.64**	3.68**
		Mattaponi	0.14	0.53	1.79*	1.00	4.13**
		Pamunkey	0.40	0.30	2.46**	1.27	7.59**
	DIC	James	0.76	1.55	1.27**	4.41**	2.50**
		Mattaponi	0.74	2.05	1.74**	2.27**	1.48**
		Pamunkey	0.68	2.10	1.30*	3.16**	1.00**
	pCO ₂	James	0.40	241	5.84**	3.48	2.38*
Mattaponi		0.82	367	3.31**	2.65**	4.14**	
Cl	Pamunkey	0.81	357	3.81**	2.73**	4.01**	
	James	0.46	24.7	6.26**	8.54**	6.97**	

917

918



919 Figure 1. Map showing USGS discharge gauging locations, estuarine sampling sites and
920 continuous dissolved oxygen monitoring locations on the Mattaponi, Pamunkey and James.
921 Inset: James and York watersheds in relation to physiographic provinces.

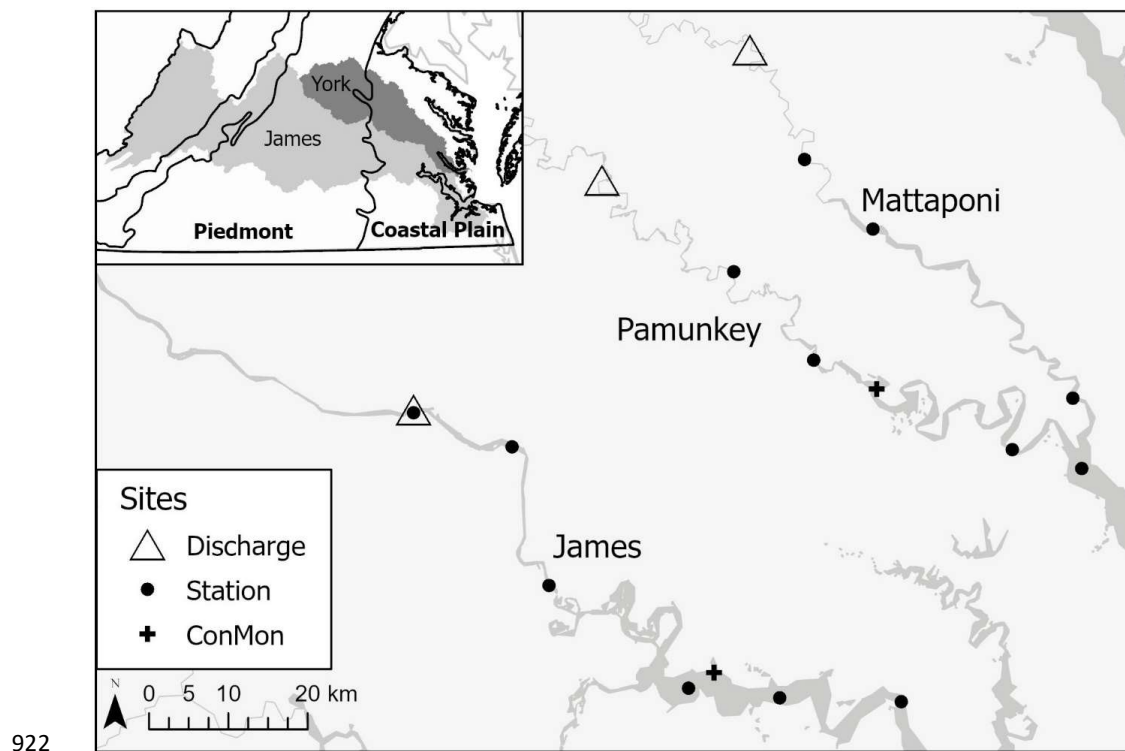




Figure 2. Seasonal variation in instantaneous discharge measured at the Fall Line of the James, Mattaponi and Pamunkey Rivers. Here and in subsequent figures, symbols denote median (bar), 25 and 75 %-tiles (box), 5 and 95 %-tiles (whiskers) and outliers (dots).

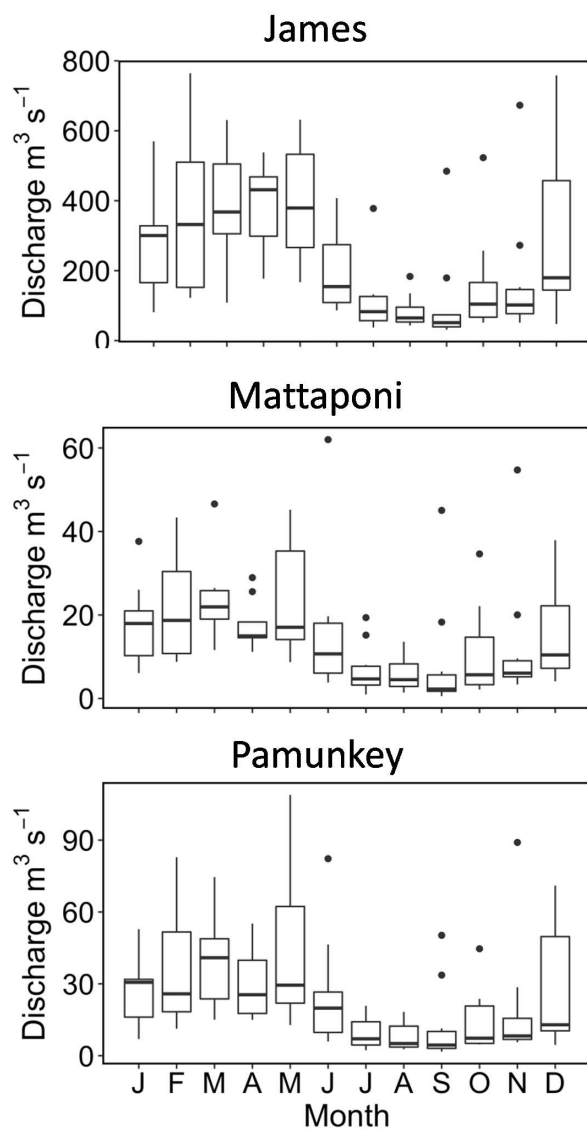


Figure 3. Time series of Cl concentrations in the tidal fresh segment of the James Estuary (upper panel) and Cl fluxes associated with river inputs, estuarine export and net tidal exchange (lower panels).

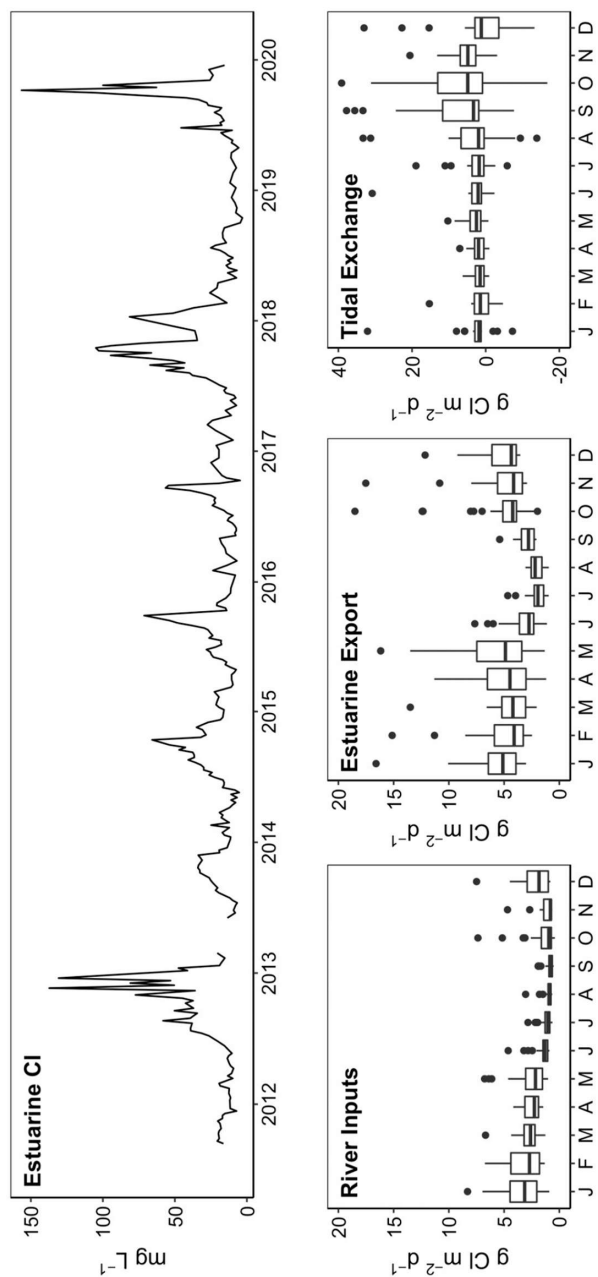




Figure 4. Results from GAM analysis depicting changes in riverine DOC, POC and DIC as a function of discharge (Q) for the James Mattaponi and Pamunkey Rivers.

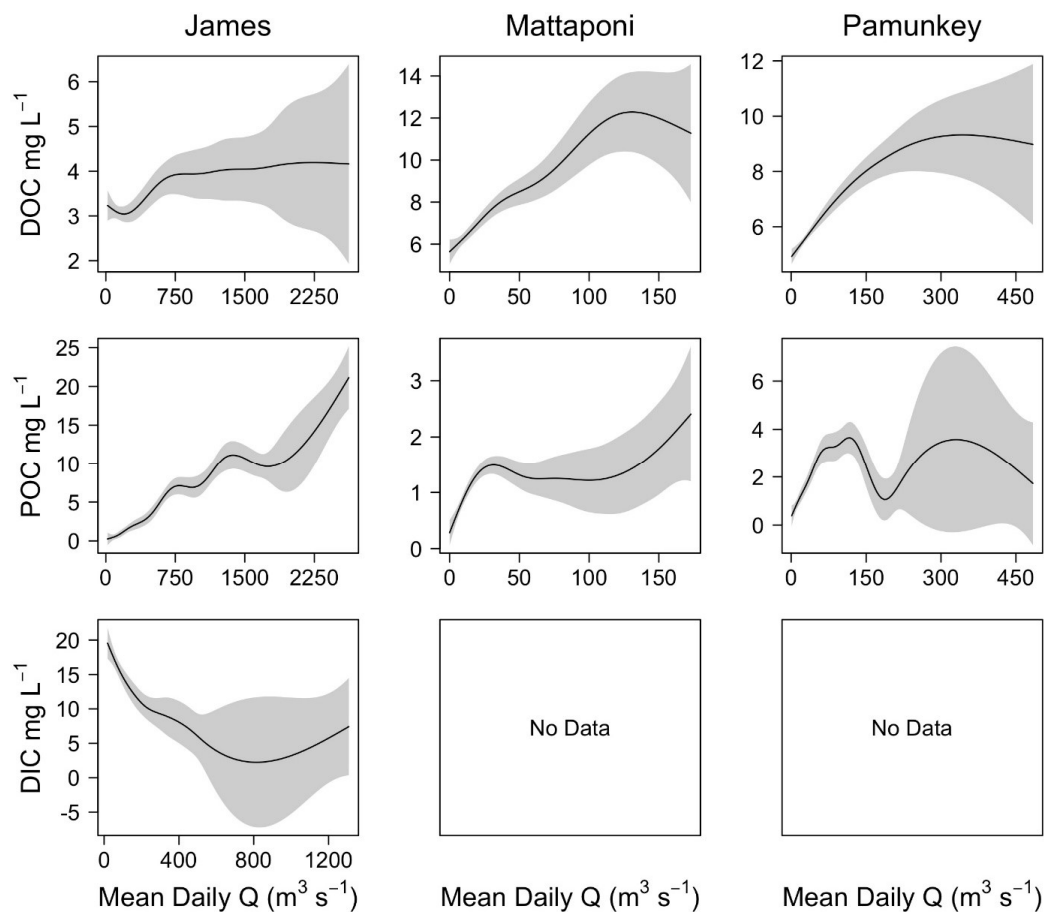


Figure 5. Results from GAM analysis depicting the effects of discharge (Q) on estuarine DOC, POC and DIC for the James Mattaponi and Pamunkey Estuaries. Concentrations are volume-weighted averages among estuarine sampling locations.

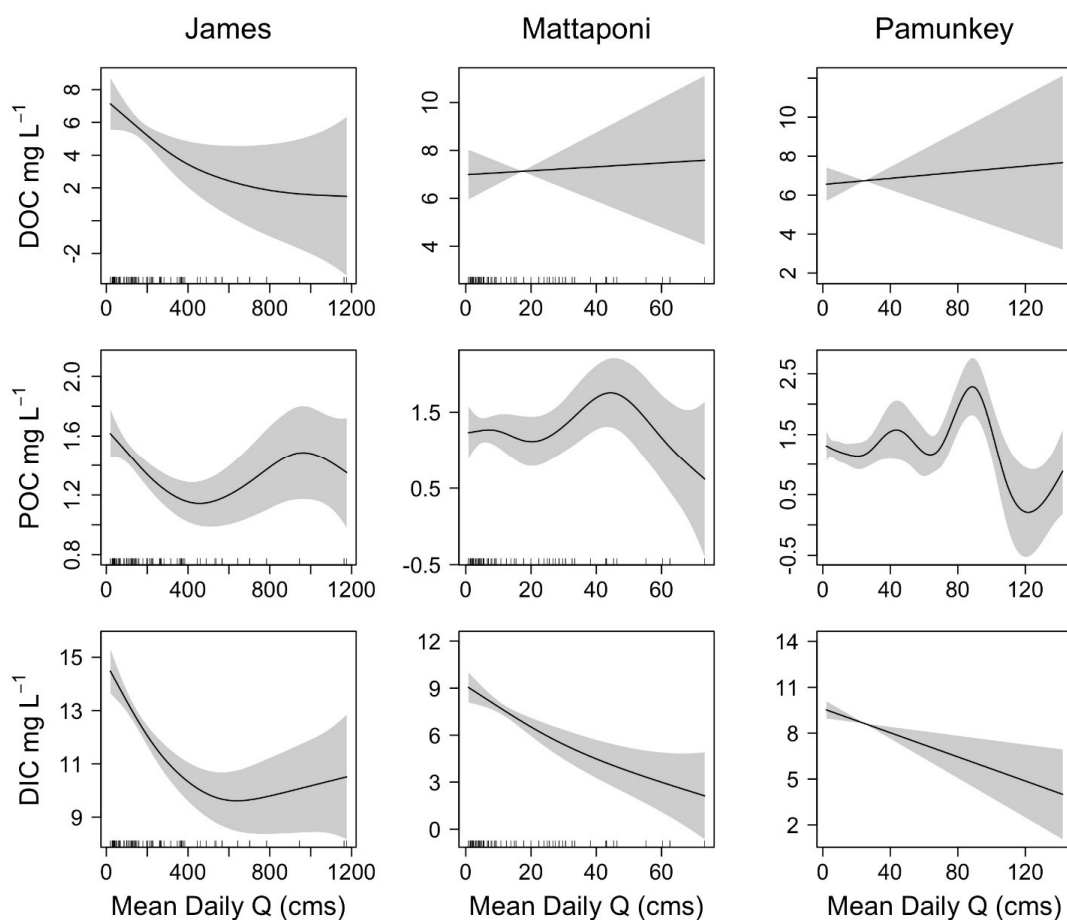


Figure 6. Results from GAM analysis depicting seasonal (day of year; DOY), inter-annual (decimal date) and discharge dependent variation in pCO₂ of the James, Mattaponi and Pamunkey Estuaries. Analyses were based on volume-weighted averages from 3-4 sampling locations in each estuary.

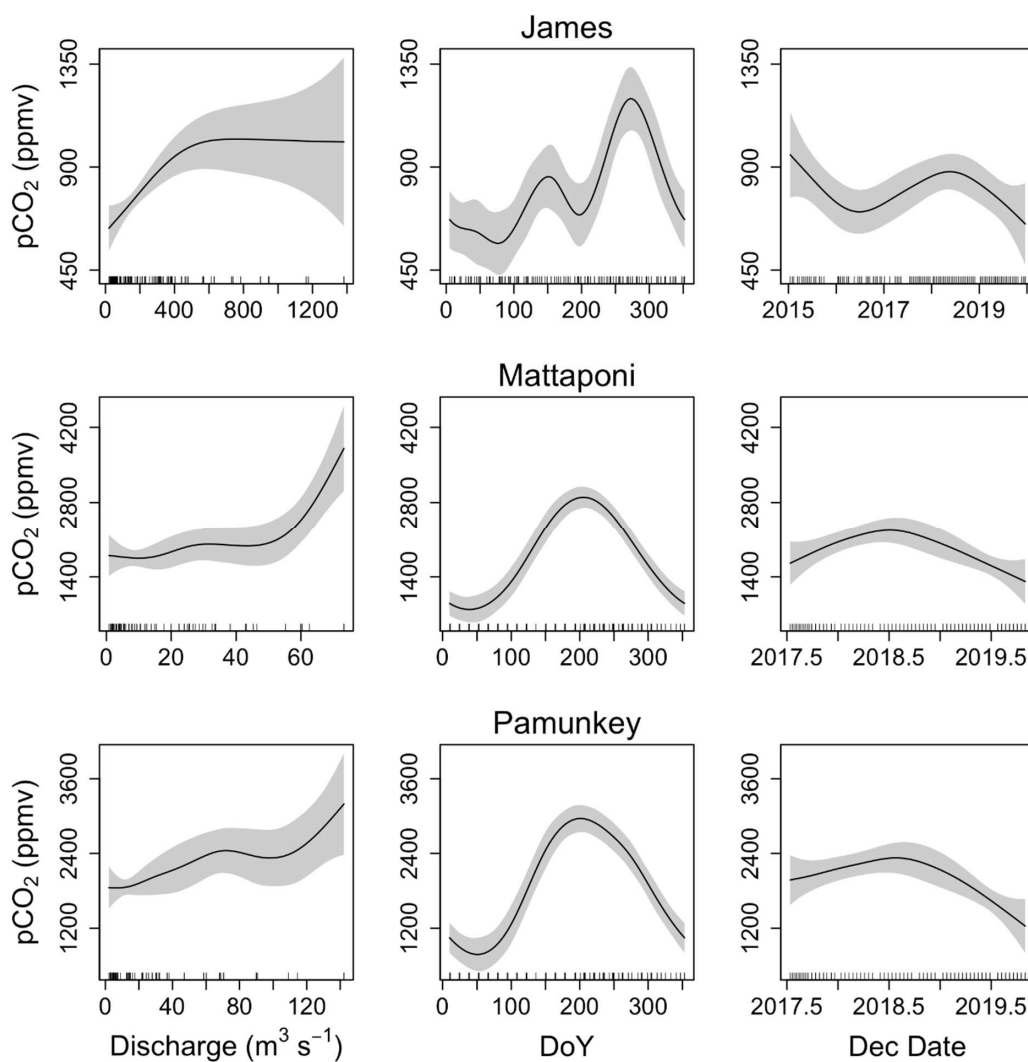




Figure 7. Monthly average values of air-water CO₂ fluxes for the James, Mattaponi and Pamunkey Estuaries. Positive values denote efflux of CO₂ from the estuary.

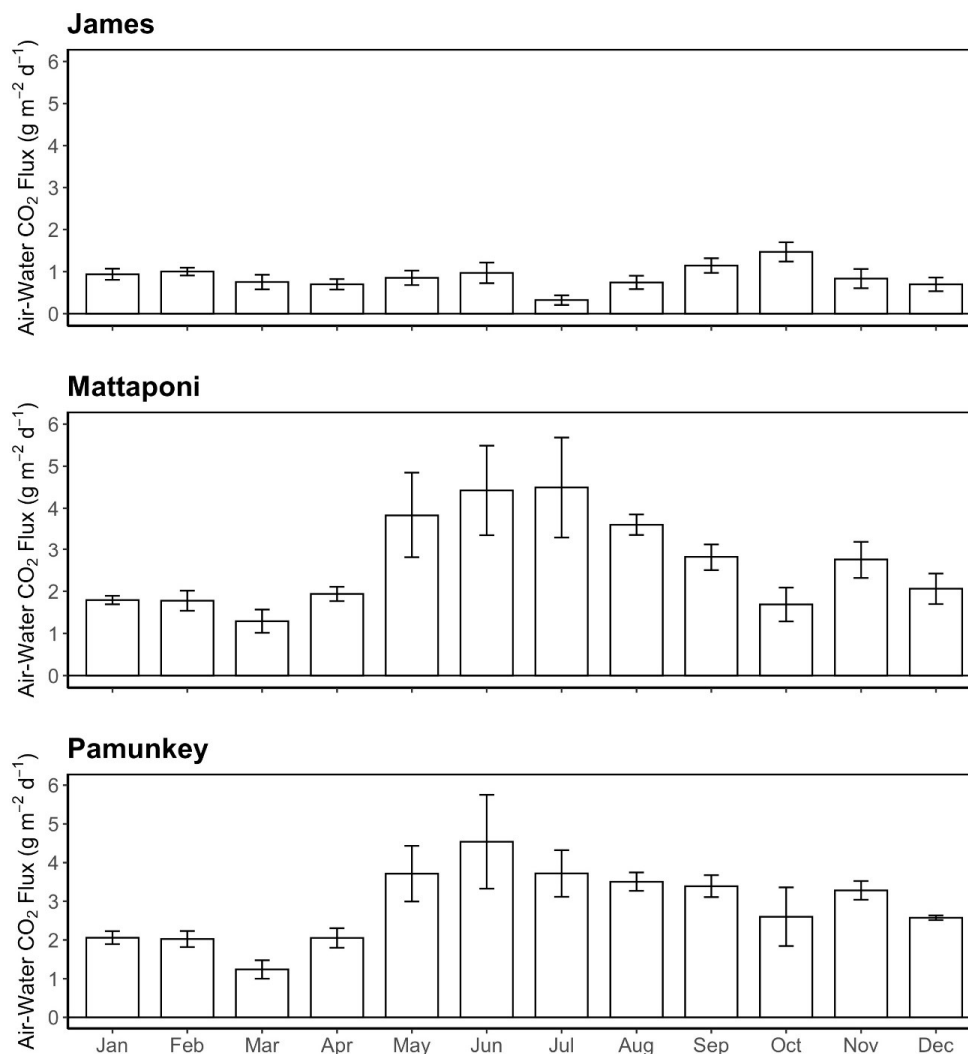


Figure 8. Seasonal variation in DOC, POC and DIC fluxes associated with riverine inputs, estuarine export, tidal exchange and estuarine retention for the tidal freshwater segment of the James Estuary (note differences in y axis scaling). Negative values for estuarine retention denote a net loss. DIC retention estimates take into account atmospheric losses of CO₂.

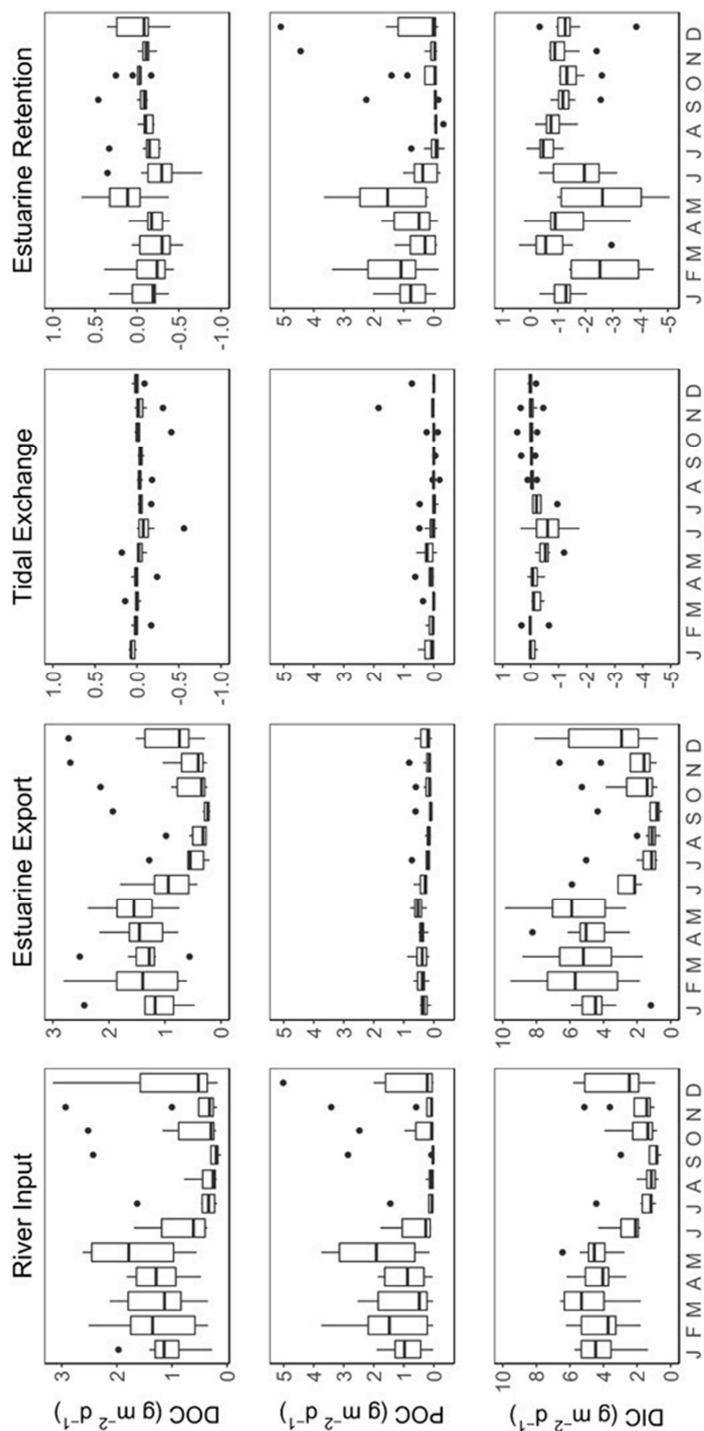




Figure 9. River input and estuarine export fluxes of DOC and POC for the Pamunkey (PMK) and Mattaponi (MPN) estuaries.

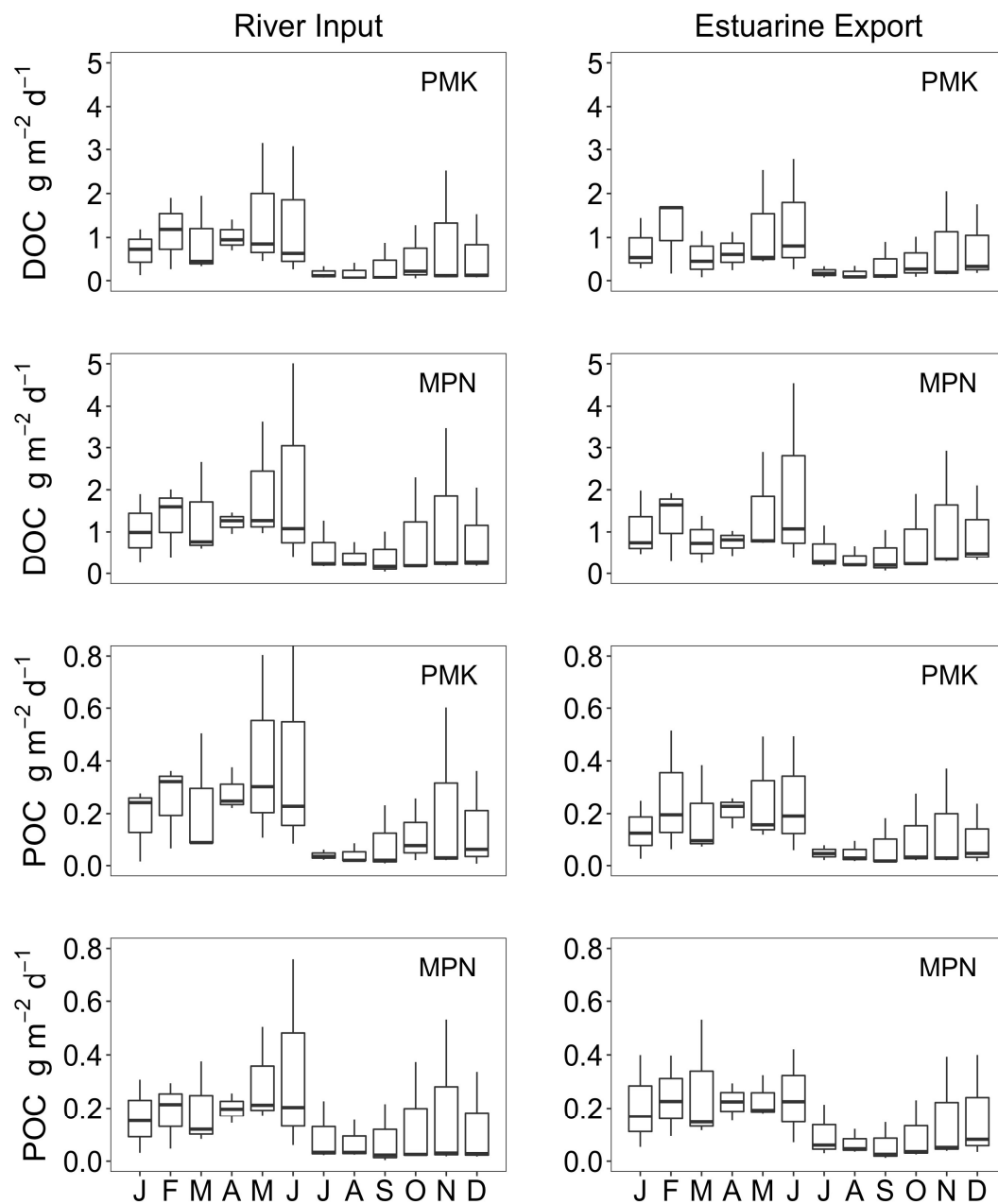
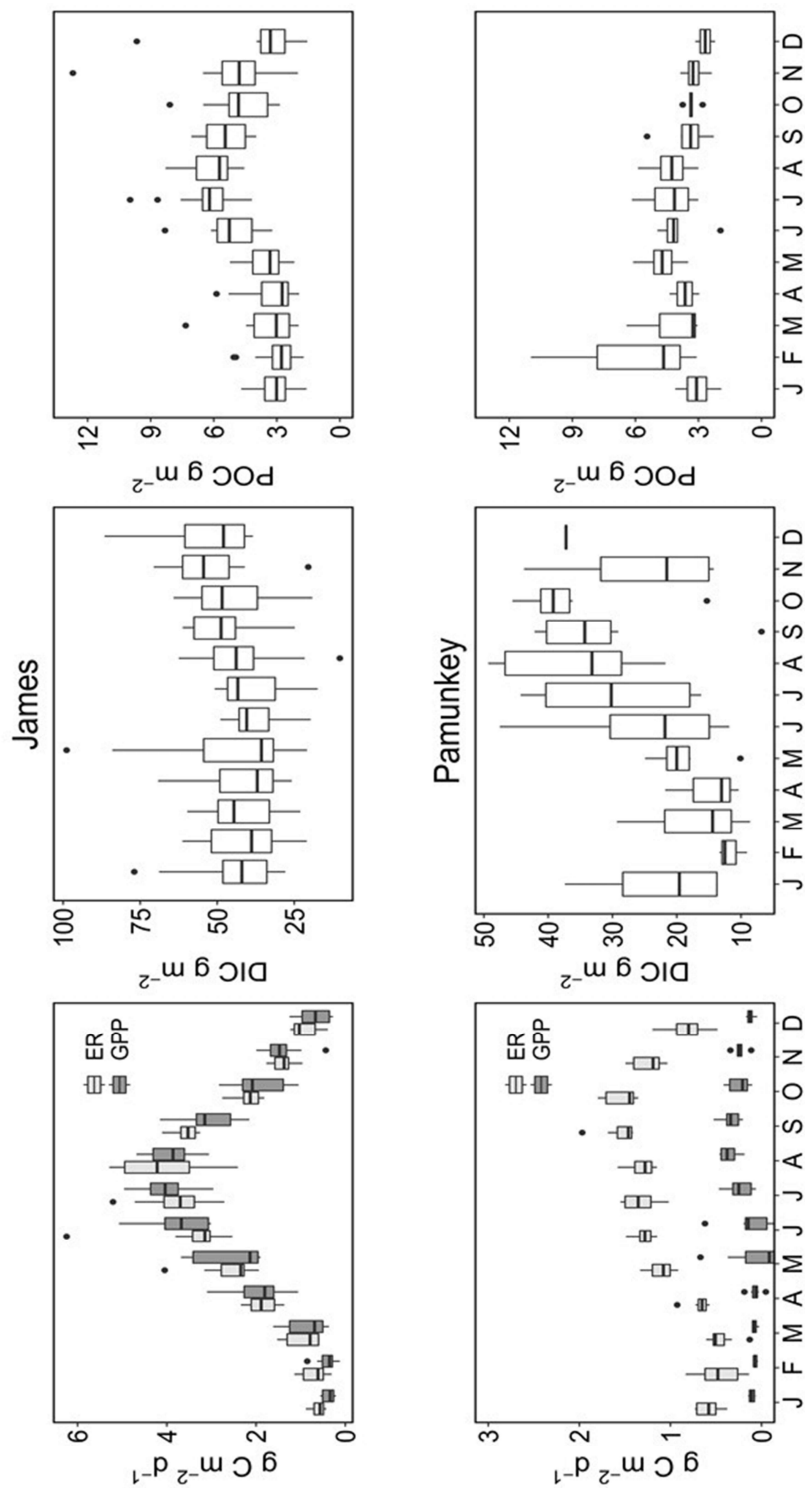


Figure 10. Seasonal variation in ecosystem metabolism (GPP and ER) in comparison to DIC and POC concentrations in the James and Pamunkey estuaries.



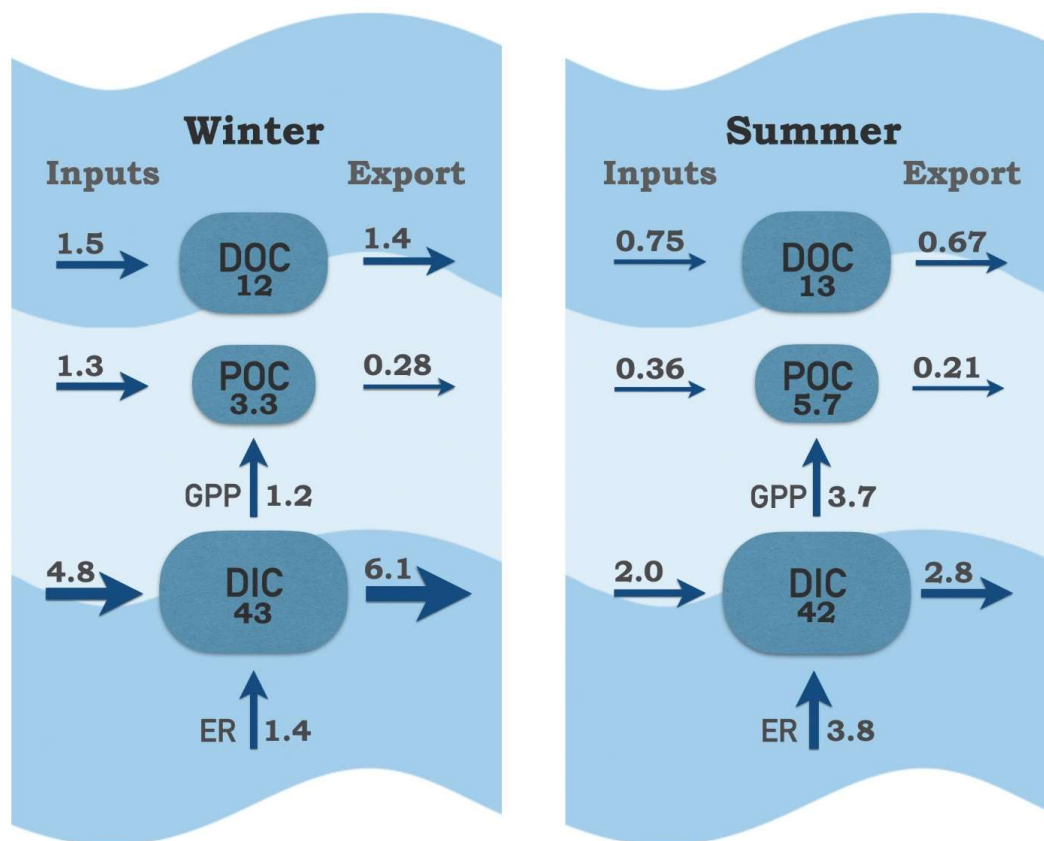


Figure 11. Carbon pools and fluxes within the tidal fresh segment of the James Estuary during winter (Jan-May) and summer (June-Sept). Inputs include riverine, local tributary and point source contributions; exports include tidal exchange and atmospheric losses of CO₂. Carbon pools (boxes) are g C m⁻²; fluxes (arrows) are g C m⁻² d⁻¹.